SAND REPORT

SAND2003-2879
Unlimited Release
Printed August 2003

Defect Reduction in Gallium Nitride Using Cantilever Epitaxy Thesis for M.S. in Electrical Engineering-University of New Mexico, May 2003

Christine C. Mitchell

Prepared by
Sandia National Laboratories
Albuquerque, New Mexico 87185 and Livermore, California 94550

Sandia is a multiprogram laboratory operated by Sandia Corporation, a Lockheed Martin Company, for the United States Department of Energy under Contract DE-AC04-94AL85000.

Issued by Sandia National Laboratories, operated for the United States Department of Energy by Sandia Corporation.

Available to DOE and DOE contractors from
U.S. Department of Energy
Office of Scientific and Technical Information
P.O. Box 62
Oak Ridge, TN 37831

Telephone: (865)576-8401
Facsimile: (865)576-5728
E-Mail: reports@adonis.osti.gov
Online ordering: http://www.doe.gov/bridge

Available to the public from
U.S. Department of Commerce
National Technical Information Service
5285 Port Royal Rd
Springfield, VA 22161

Telephone: (800)553-6847
Facsimile: (703)605-6900
E-Mail: orders@ntis.fedworld.gov
Online order: http://www.ntis.gov/ordering.htm

SAND 2003-2879
Unlimited Release
Printed August 2003

Defect Reduction in Gallium Nitride Using Cantilever Epitaxy

Thesis for M.S. in Electrical Engineering – University of New Mexico, May 2003

Christine C. Mitchell
Chemical Processing Sciences
Sandia National Laboratories
P.O. Box 5800
Albuquerque, NM 87185-0601

ABSTRACT

Cantilever epitaxy (CE) has been developed to produce GaN on sapphire with low dislocation densities as needed for improved devices. The basic mechanism of seeding growth on sapphire mesas and lateral growth of cantilevers until they coalesce has been modified with an initial growth step at 950°C. This step produces a gable with $(11\bar{2}2)$ facets over the mesas, which turns threading dislocations from vertical to horizontal in order to reduce the local density above mesas. This technique has produced material with densities as low as 2-3x10^7/cm^2 averaged across extended areas of GaN on sapphire, as determined with AFM, TEM and cathodoluminescence (CL). This density is about two orders of magnitude below that of conventional planar growths; these improvements suggest that locating wide-area devices across both cantilever and mesa regions is possible. However, the first implementation of this technique also produced a new defect: cracks at cantilever coalescences with associated arrays of lateral dislocations. These defects have been labeled "dark-block defects" because they are non-radiative and appear as dark rectangles in CL images. Material has been grown that does not have dark-block defects. Examination of the evolution of the cantilever films for many growths, both partial and complete, indicates that producing a film without these defects requires careful control of growth conditions and crystal morphology at multiple steps. Their elimination enhances optical emission and uniformity over large (mm) size areas.

ACKNOWLEDGMENTS

This research would not have been completed without the efforts of many people at Sandia National Laboratories. Among those who have been instrumental in my growth as a scientist I would like to thank Mike Coltrin, Dan Koleske, Nancy Missert, David Follstaedt, and Andy Allerman.

I would like to give a special thank you to Isak Reines and Daniel Derkacs who completed student internships as undergraduate students from UNM EECE department working on the data collection and processing for this project under my supervision.

In addition, I have had the help and guidance from many people with experience in processing. Andrea Ongstad, Karen Cross, Kate Bogart, Leo Griego, Ron Briggs, Jeanne Sergeant, and Carol Ashby have all contributed to the processing portion of this project over the last 3 years.

The selective area growth and GaN kinetic studies were done in collaboration with Michael Coltrin.

Nancy Missert and Guild Copeland have been instrumental in helping me learn the skills necessary to collect accurate cathodoluminescence spectra and have provided valuable knowledge and expertise to the analysis of these special materials.

David Follstaedt, Paula Provencio, Michael Moran and Adam Norman have completed all of the TEM sample preparation and analysis for this project and their work is greatly appreciated.

Steve Lee provided valuable instruction and advice on x-ray diffraction measurements of cantilever films.

I would also like to extend a huge thank you to Billie Kazmierczak who keeps our department at Sandia on even keel and operating efficiently.

I would like to take this opportunity to thank my committee at UNM Dr. Tom Sigmon, Dr. Ralph Dawson, and Dr. Diana Huffaker, you have been generous with your time and have helped make this Sandia sponsored project a successful UNM master's thesis.

This research was supported by Sandia National Laboratories, a multiprogram laboratory operated by Sandia Corporation, a Lockheed Martin Company, for the United States Department of Energy under contract DE-AC04-94L85000.

Finally, and most importantly, I would like to thank my husband, Bill, and my parents. They have always supportive in everything I choose to pursue.

TABLE OF CONTENTS

List of Figures

List of Tables

Chapter 1: Introduction

This thesis is a continuation of a project started by Carol Ashby, Dave Follstaedt, Jung Han (now at Yale University), and myself. It will cover a technique called cantilever epitaxy, which is an adaptation of selective area growth for GaN. The cantilever epitaxy technique uses patterned sapphire substrates to define regions from which lateral overgrowth can occur, as shown in Figure 1. This technique is effective in reducing threading dislocations in GaN by more than an order of magnitude. The original idea has been filed to the U.S. patent office under application number 09-754803, *Cantilever Epitaxial Process.*

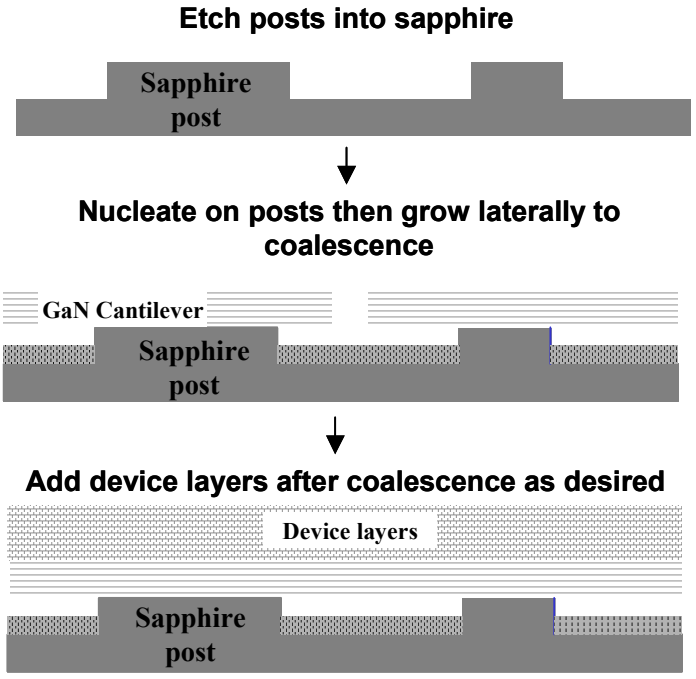

Figure 1. Schematic of basic cantilever epitaxy process. Nucleation and growth of GaN occurs directly on an etched sapphire substrate.

1.1 Background

Gallium nitride (GaN) is receiving significant attention because of its favorable and unique combination of optoelectronic, microelectronic, piezoelectric, mechanical, and chemical properties. GaN has a bandgap of 3.4 eV, strong piezoelectric fields in c-plane GaN, and is chemically inert. These properties make GaN suitable for, among other things, LEDs and lasers that emit in the blue and UV regimes, high temperature, power, and frequency electronics for use in adverse environments, and mixed opto-mechanical-electronic devices for multifunctional integrated microsystems. Because single crystal GaN substrates are not readily available, GaN is often grown on sapphire or SiC substrates. The hexagonal crystal structure of these substrates forms a template for oriented growth of GaN, but their large lattice mismatches with respect to GaN (13.5% and 3.3%, respectively) lead to high densities of vertical threading dislocations (VTDs) that propagate to the surface during growth. Dislocation densities as high as 10^9 VTDs/cm^2 are not uncommon.

These threading dislocations are the cause of great consternation among the GaN growth community. Initially it was thought that no functioning device could be made on material with the enormous number of dislocations in GaN grown in this way [1]. Despite this limitation many successful laser diodes in the blue and green regime have been fabricated on material grown by lateral epitaxial overgrowth (LEO), with lifetimes greater than 10000 hours. Unfortunately, high dislocation density ultimately limits the full potential for GaN-based devices. In general, devices will have longer lifetimes, more reliable performance, and greater efficiency if dislocations can be reduced.

GaN epitaxial growth can be done either by metal organic chemical vapor deposition (MOCVD), molecular beam epitaxy (MBE), or hydride vapor phase epitaxy (HVPE). The experiments discussed in this thesis have all been completed via MOCVD. The growth is started with a standard two-step sequence that involves a low-temperature (LT) nucleation layer grown at ~550 °C followed by a high temperature layer grown at ~ 1050 °C. Variations on these growth steps, especially the LT nucleation layer and the recovery period from low to high temperature, can greatly affect the quality of the material, dislocation density, and subsequent brightness of UV LEDs [2].

The MOCVD reactor used for these experiments is a custom fabricated high-speed rotating disk design that has RF heating, water-cooled quartz walls, and quartz windows that allow in-situ optical access. The metal organic precursor used is trimethylgallium (TMG). The nitrogen source is ammonia (NH_3) that is purified by an Aeronex Gate Keeper purifier. The carrier gas is hydrogen, which is purified with a Matheson H_2 Nanochem purifier.

In addition to improvements in the way planar growth is done, selective area growth (SAG) methods have been employed to improve the material quality. SAG is a well-proven concept that has been used in the growth of many III-V semiconductors [3]. This concept was adapted to GaN with great success.

1.2 Selective Area Growth for GaN

SAG is known by many names within the GaN community. Two of the most common are lateral epitaxial overgrowth (LEO) or epitaxial lateral overgrowth (ELO). These methods use a GaN layer 1-3 μm thick that has been grown by MOCVD on a

sapphire or SiC substrate. At this point the substrate is taken out of the reactor and a layer of SiO_2 or Si_3N_4 is deposited using plasma enhanced chemical vapor deposition (PECVD). This layer is generally 100 nm thick. The dielectric layer is patterned with standard photolithography techniques and openings in the dielectric material are etched using reactive ion etching (RIE). Studies with AFM of the surface before and after the etch show no adverse effects. The growth then proceeds through openings in the mask of SiO_2 or Si_3N_4. This growth initially occurs vertically until the growth exceeds the thickness of the mask, where after lateral overgrowth occurs. ELO can be obtained under a range of growth conditions, and is affected by the V/III ratio, pressure, temperature and orientation of the mask with respect to the underlying GaN. The advantage of SAG is that the VTDs in the base planar film, generally on the order of 10^9 dislocations/cm^2, propagate through the opening but are blocked and not found in material grown over the mask, leading to lower overall densities and areas that have dislocation densities as low as 10^6 VTDs/cm^2 [4-7]. The best GaN devices are often grown on ELO base layers. A disadvantage of ELO is that it requires two growth steps, which can be expensive and time consuming. In addition, the mask can cause unintentional doping of the overgrown GaN (Si is a commonly used n-type dopant, while O is an unwanted impurity).

Another alternative to SAG is called pendeo epitaxy [8] where mesas and trenches are patterned and etched into a GaN grown on a planar substrate; these substrates have traditionally been SiC. The resultant substrate has GaN posts adjacent to newly exposed SiC substrate in the trench. Material is grown laterally from the GaN mesas over the trenches to obtain low VTD density. This method is especially effective for SiC substrates because after the patterned substrate is etched growth can be continued without

a subsequent nucleation layer. This allows for selective growth on the previously grown GaN without growth on the newly exposed SiC substrate. This process can be performed without a dielectric mask. The disadvantage to this growth process is that, like ELO, it requires two growth sequences, in addition to the processing.

An alternative lateral growth method, cantilever epitaxy (CE), has been developed to remove and redirect VTDs [9]. With CE, the substrate is first patterned with mesas and trenches, and then GaN is nucleated on the mesa and laterally grown over the trenches using the aforementioned two-step growth process. This method has the advantage of requiring only one growth sequence, since the substrates themselves are patterned and etched rather than needing a pre-grown base layer. The work presented here focuses on CE growth on sapphire while others have used similar methods with Si and SiC substrates [10, 11].

Before developing the cantilever epitaxy process, a significant amount of time was spent understanding GaN growth kinetics using ELO. From this study the growth specific reaction rates of the various GaN facets were measured as a function of several growth parameters. This information is used to guide the selection of growth conditions for cantilever epitaxy, especially those needed for advanced dislocation reduction techniques. These studies included detailed research on the fundamental kinetics independent of mask design or fill-factor. As was mentioned earlier, one significant factor in the reaction rates of predominate faces in GaN ELO is the orientation of the lines with respect to the underlying GaN. Lines oriented in the $[1\bar{1}00]$ direction, with respect to the underlying GaN, will show (0001), $(11\bar{2}2)$, and $(11\bar{2}0)$ faces, while lines oriented in the $[11\bar{2}0]$ direction will show (0001) and $(1\bar{1}01)$ faces. Figure 2 shows a

schematic illustrating the common faces for both directions of lines. The sapphire used for all of these experiments is a-plane sapphire. For this substrate and standard MOCVD growth conditions, the GaN grown is always c-plane; it grows with the c axis perpendicular to the substrate.

Reaction rate constants help define the rate at which each face grows. For a heterogeneous surface reaction, the rate of progress of a reaction, q, is defined by equation 1,

$$q_i = k_i[A]^a[B]^b \qquad \text{Eq. (1)}$$

where k_i is the reaction rate constant of the face in question, [A] and [B] are the concentration of reactants. The units of q are $\left(\frac{mol}{cm^2 * \sec}\right)$. For gallium nitride the limiting reactant is Ga so equation 1 condenses to the form seen in Equation 2,

$$q_i = k_i[Ga] \qquad \text{Eq. (2)}$$

where the [Ga] is the concentration of gallium in the gas phase at the surface. The units of [Ga] are $\left(\frac{mol}{cm^3}\right)$. From these two equations it is seen that the units on k_i must be $\left(\frac{cm}{\sec}\right)$. Equation 3 shows how the rate of progress of the surface, q, can be used to determine the growth rate,

$$G.R. = q_i * \frac{1}{\rho_{solid}} * M.W \qquad \text{Eq. (3)}$$

where G.R. is the grown rate in $\frac{cm}{\sec}$, ρ_{solid} is the density of the material, and M.W. is the molecular weight of the material. Therefore, the growth rate of any face depends both on the reaction rate constant and the concentration of precursor. Figure 3 shows the

variation in specific reaction rates for the (0001), $(11\bar{2}2)$, $(11\bar{2}0)$, and $(1\bar{1}01)$ faces as a function of temperature for a constant V/III ratio. This graph depicts how the growth rates of the various faces change with respect to each other. For example, as the temperature is increased from 1050 °C to 1080 °C the growth rates of the $(11\bar{2}2)$ and $(11\bar{2}0)$ faces increase with respect to the growth rate of the (0001) face. This change in reaction rate produces a change in shape in the overgrowing material. During growth at 1080 °C the $(11\bar{2}2)$ face grows itself to extinction and the $(11\bar{2}0)$ face propagates faster than the basal plane. This difference in relative growth rates produces a line with a rectangular cross-section. At low temperatures the reaction rates change, and this is manifested as a shape change in the overgrowing ELO feature cross-section. The basal plane or (0001) face has a faster growth rate compared to the $(11\bar{2}2)$ and $(11\bar{2}0)$ faces, yielding a triangular feature shape. The cantilever epitaxy substrate posts are patterned in the $[1\bar{1}00]$ direction, with respect to the GaN that will be grown, due to the comparatively fast growth rates of the $(11\bar{2}2)$ and $(11\bar{2}0)$ faces.

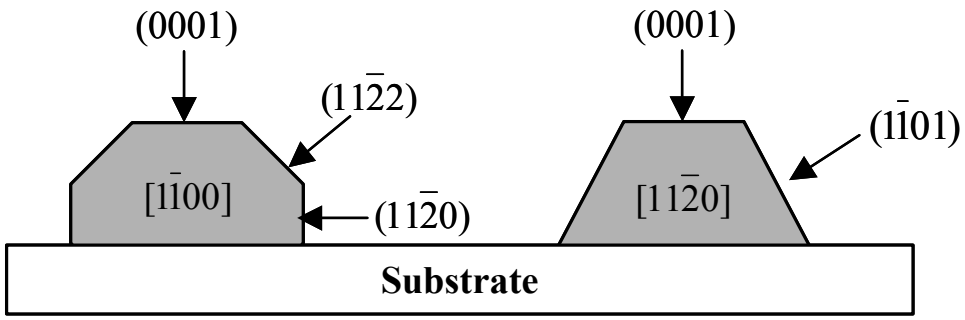

Figure 2. Schematic of common faces for ELO lines orientated in the $[11\bar{2}0]$ and $[1\bar{1}00]$ directions

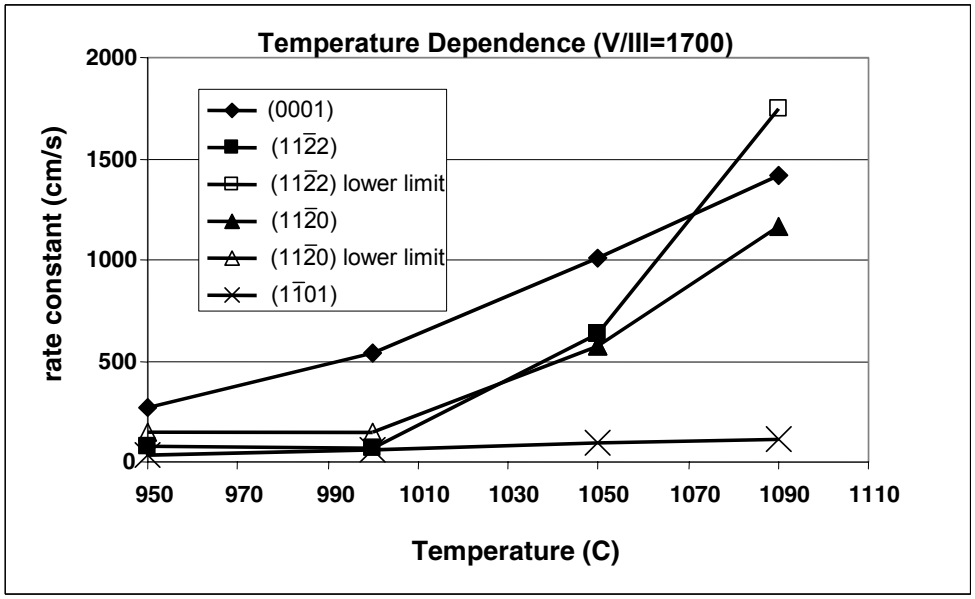

Figure 3. Graph of rate constants for the four primary faces in ELO and cantilever epitaxy. Knowing the variation of the rate constants with temperature helps in determining the growth conditions needed to accomplish desired stages of cantilever epitaxy.

Chapter 2: Substrate Preparation

2.1 Sapphire Processing

One unique feature of CE is that all of the substrate modification needed for the growth is done on bare sapphire substrates. For this thesis, all experiments are conducted on double side polished sapphire substrates with a thickness of 17 mils. This preparation is not trivial and many talented processing and etching specialists have given valuable advice and assistance. In addition, great care is taken to assure that the wafers are well characterized before growth occurs. This is essential to being able to understand the results of any particular growth step.

Processing of the substrate begins with a clean double-side-polished sapphire wafer. After inspection, the first of four masking layers is spun onto the wafer. Due to the difficulty of removing hard-baked photoresists (HBPR), an initial layer of Polymethylglutarimide (PMGI) is spun onto the wafer at 4000 rpm for 30 seconds and baked twice. Baking PMGI ensures that all solvents will be driven out. The estimated thickness of this layer is around 0.5μm. The second and most robust layer of the mask is a viscous layer of Clariant AZ5740 photoresist (PR). This particular photoresist has been found to better withstand the high-density plasma used later to etch the sapphire. The 5740 is spun at 1300 rpm for 30 seconds in a Gyrset spinner. Under these conditions the resist initially spins on at ~ 11 μm thick. The sapphire substrates are not beveled, as is common in silicon substrates, and as a result a build up at the edge of the wafer, called an "edge bead" occurs. Immediately following this spin, an edge bead removal is done using a Shipley edge bead removal (EBR) solvent at a speed of 1000 rpm. The wafer is

then initially baked for 5 minutes at 110°C. This is followed with a hard-bake in a convection oven at 190°C for 1 hour. This acts to slowly ramp the temperature of the photoresist to prevent bubbles from forming on the surface. An alternate way of removing the edge-bead is to expose the PR to UV light, in the same way you would expose a pattern, and then develop with an alkaline-based developer, such as Shipley 421K. This method produces significantly more bubbles in the final hard-baked layer, which results in greater non-uniformity both over a single 2" wafer and from wafer to wafer. After the hard bake, a 0.5 μm thick Si_xN_y layer is deposited atop the 5740. As will be seen later, the Si_xN_y is the mask for the electron cyclotron resonance (ECR) etch of the HBPR layer. A Plasma-Therm 790 Plasma Enhanced Chemical Vapor Deposition (PECVD) machine deposits the Si_xN_y. The plasma is induced from a gaseous mixture of 120-sccm silane (SiH_4), 4.1-sccm ammonia (NH_3), and 160-sccm nitrogen (N_2). A 45 W, 13.56 MHz RF source strikes the plasma on a 250°C substrate heater and deposits at a rate of 70-90 Å/min.

The final layer of the mask is a layer of Clariant AZ9245 or AZ4110 photoresist, called the patterning resist. This resist acts as a mask for the Si_xN_y etch. Before this layer is spun, hexamethyldisilazane (HMDS) is introduced to the wafer in a chamber specifically designed for this process. Problems with photoresists not sticking to or "wetting" the surface occur when the wafer is hydrophilic and the resist is hydrophobic. This is the case with PR on SiO_2 or SiN. Lasting 33 minutes, the process initially heats the wafer and allows the gas-phase HMDS to react with the surface OH groups in a process known as silylation. This process essentially lowers the surface energy of the wafer surface thereby allowing a higher molecular contact angle and greater surface area

coverage. Immediately after the vapor HMDS process the layer of 9245 patterning resist is spun at 4000 rpm for 30 seconds and baked at 110°C for 2 minutes. No edge bead removal is required at this step because the edge bead removal for the previous thick resist results in a beveled edge. The wafer is exposed for 18 sec and developed in Shipley 1:4 400K developer until the pattern is visibly recognizable and no visual diffraction atop the wafer is present. At this point the mask layers are fully deposited and the wafer is ready for the etching. Figure 4 shows a schematic of the final masking structure prior to any etching steps.

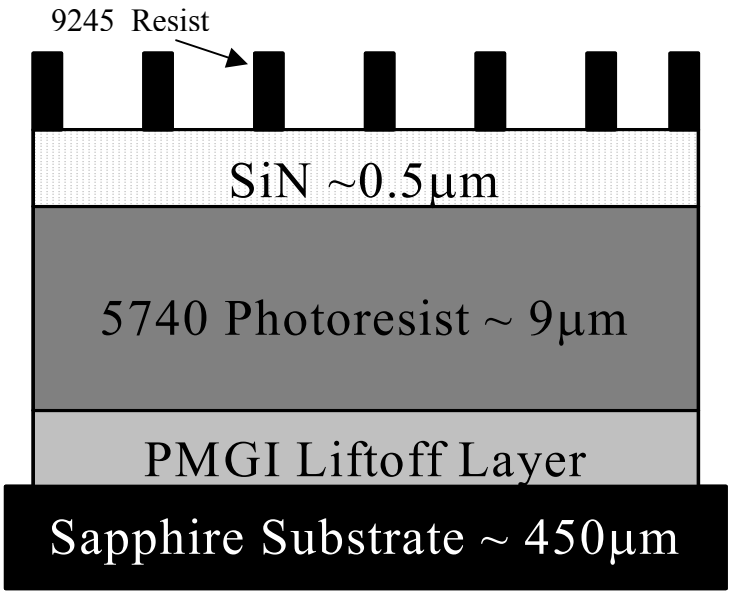

Figure 4. Schematic of the quad-level mask used to process the sapphire substrates for cantilever epitaxy.

A Plasma-Therm Batchtop Reactive Ion Etch (RIE) is used to remove the Si_3N_4 layer not covered by the patterning photoresist layer. The Batchtop uses a sulfur hexafluoride (SF_6) and Oxygen (O_2) based plasma. The etch time is determined in-situ by detecting the reflection off of a silicon partner piece run simultaneously with the

original deposition of Si_xN_r. The remaining 9245 photoresist is removed via an acetone spray gun. This leaves the SiN_x as a mask for the HBPR etch.

The electron cyclotron resonance (ECR) etch is a very important step pertaining to the final outcome of the wafer. The ECR etch has the primary purpose of removing the hard-baked 5470 layer without disturbing the SiN layer. It is very easy to over etch the resist at this point and destroy the wafer. The aspect ratio of features for the HBPR etch is approximately 7:1 and the width of the mask that ultimately defines the sapphire posts is 1.5 μm. A common etching time is around 10 minutes, but can vary depending upon the etch chamber condition. The final step in the process is to etch the desired sapphire posts. An extremely high-density low-energy Inductively Coupled Plasma (ICP) etch is used. A 13.56 MHz power source generates a magnetic field that inductively couples electrons from argon and boron trichloride (BCl_3), causing them to circulate and ionize other molecules creating the plasma. The electric field of the RF source is shielded from the plasma to avoid capacitive coupling, which can lead to high-energy plasma. The 70-minute ICP etch attacks the entire surface of the wafer so the depth and uniformity of the sapphire posts is determined by the robustness of the remaining mask. Figure 5 shows the three primary steps needed for etching a sapphire substrate. The 9245 or other patterning resist acts as a mask for the Si_xN_y etch, the Si_xN_y acts as a mask for the HBPR etch, and the HBPR acts as a mask for the sapphire etch.

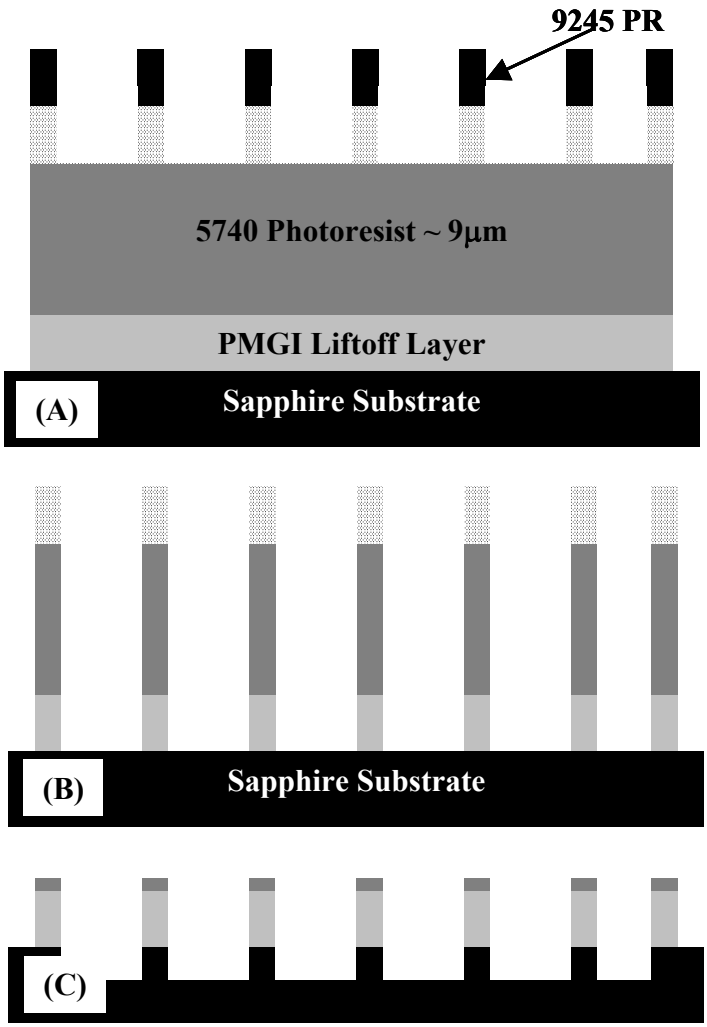

Figure 5. This figure shows the three main steps for etching a CE sapphire substrate. (A) The 9245 PR acts as a mask for the Si_xN_y etch. (B) The Si_xN_y acts as a mask for the HBPR etch. (C) The HBPR acts as a mask for the sapphire etch.

In a final processing stage, the wafer must be cleaned. Reminiscent mask and mounting agent (MUNG) are removed by soaking the wafer for 10 minutes in an oxidizing solution of 3:1 H_2SO_4:H_2O_2. This "piranha" clean exothermically reacts, and effectively removes the overlying mask. Any remaining MUNG on the back of the wafer can be removed manually with cotton swabs and toluene. The wafer is thoroughly rinsed

with acetone, methanol, and de-ionized water and blown dry with nitrogen. Figure 6 shows a SEM of a cantilever epitaxy substrate of 1 μm post tops with a 7 μm pitch that are 2-3 μm deep.

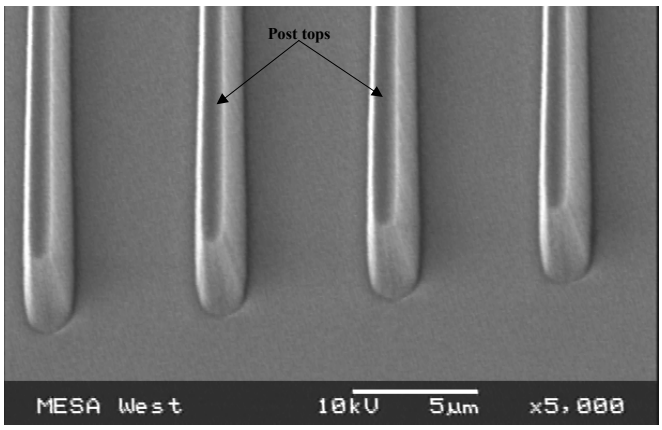

Figure 6. SEM of a cantilever epitaxy substrate after processing and prior to growth.

2.2 Substrate analysis

Inspection of the wafer after the cantilevers are patterned provides essential information needed to correlate growth conditions to the starting CE substrate. To collect the data, three tools are used: a JOEL 5800 Scanning Electron Microscope (SEM), an Alphastep profilometer, and a WYKO optical profiler. All three of these instruments are used to collect collaborative data in an effort to qualify each wafer before growth. Proper post depth is necessary to prevent the GaN growing on the bottom substrate from interfering with the laterally coalescing fronts. In addition, the top width of the posts is important to know so that the growth time to achieve pyramidal shaped GaN growth can be determined. The goal is to have completely uniform depth and top widths for all of the posts on the wafer.

The Alphastep profilometer has a stylus that is brought down to the surface of the wafer and is scanned across a series of Dek-tak pads. Dek-tak pads are larger and more widely spaced posts incorporated in the lithographic pattern for depth measurements. The stylus is wider than the 5 μm separating the real posts so it is necessary to include these pads for measurment purposes throughout the masking and etching process. This system accurately measures the depth of the pads, but is an inaccurate measure of the depth between the posts due to aspect ratio dependant etching. Simply said, as the ratio of etched to unetched area (fill-factor) changes so does the etch depth. Current dek-tak depths are on the order of 3.5 μm while the actual posts depths are only 2.5 μm. The difference between the dek-tak measurements and the actual post depth is generally 1 μm for typical etch depths. For this reason, the dek-tak measurements give an easy, quick way to measure the etch depth before more extensive measurements are taken with a non-contact white light profilometer (WYKO).

The second data collection method used to characterize the wafers is the JOEL 5800 SEM. Images taken directly above the posts (i.e. plan-view) provide a 2-dimensional image used to determine the top and bottom widths of the posts. The current goal is to have uniform top width nearing 1 μm. In addition, it is necessary to ensure that the tops of the posts are completely flat, requiring that the mask remains over the posts through the entire ICP etch. Due to the great amount of time it takes to use the profilometer and the SEM, a new method of surface profiling has been incorporated into the process.

The WYKO optical profilometer uses interference patterns created by topographical changes to create a digitized image of a selected area. The WYKO has a

fully automated stage that has been programmed to collect 47 different samples systematically located throughout the wafer. It effectively collects height data and bottom post width data but, to this point, the top post width cannot be extracted exclusively. Data points are exported in a text file format which can then be imported into Excel for graphing or other analysis. Figure 7 shows a representative plot of the height data collected from the WYKO white light profilometer. The entire 2 inch substrate can be mapped and the actual depth of the trenches can be monitored. This data has been compared to cross-section SEM data for several wafers and the measurements agree to within 10%.

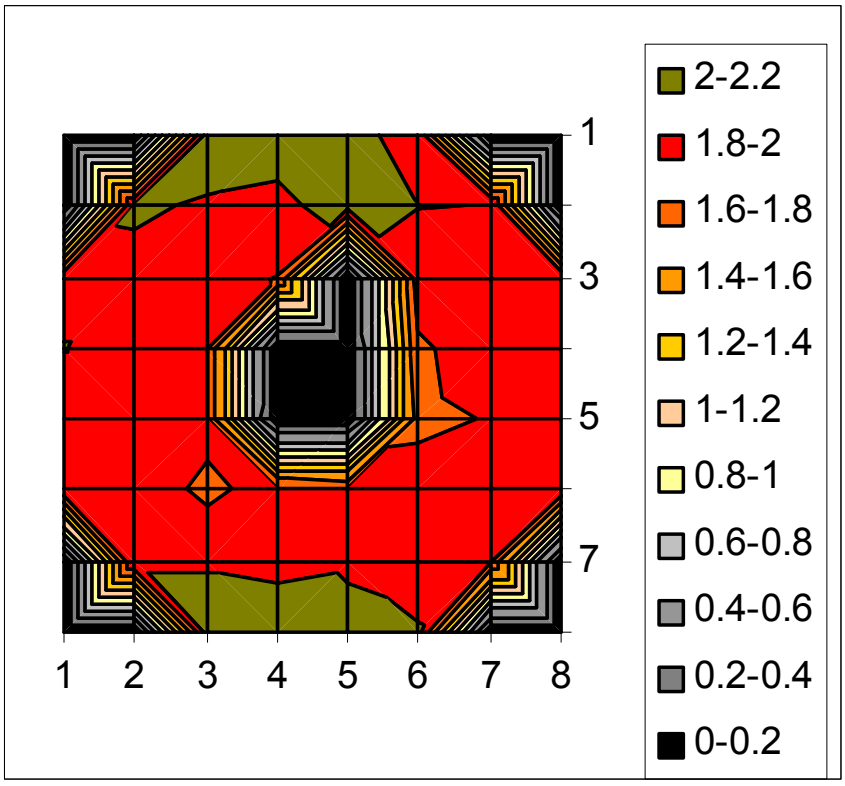

Figure 7. An excel plot of height measurements collected using they WYKO white-light profilometer.

Chapter 3: GaN Material Analysis Techniques

3.1 In-situ reflectance monitoring

In-situ optical reflectance monitoring is a method from which both optical constants and growth rates may be simultaneously extracted from the normal incidence reflectance of a growing thin film [12]. In addition to the optical constants and growth rates, this method is routinely used to measure and control the nucleation layer thickness in GaN, as well as the transition from 3D island growth to 2D coalesced planar growth. For optical reflectance to work with the CE wafers, a planar unetched region in the center of the wafer is necessary. This reduces the yield of the substrates, but this loss is acceptable considering the additional control and monitoring capability provided by optical reflectance. Practically speaking, a software program called Thermogrow is used to collect and analyze both the optical reflectance and thermal emission data. This technology was developed at Sandia Labs by Bill Breiland and Larry Bruskas and has since been patented and transferred to Thermo Oriel.

Optical probes are a good choice for in-situ monitoring of thin film growth because they are non-perturbing, can be located outside the deposition chamber, and utilize well-understood models of light and matter for measurement of thin film materials properties. In the case of MOCVD, the high pressure, high temperature, and chemically reactive deposition environment make this technique the only viable in-situ option. The reflectance beam enters and exits the system through a single port at the top of the reactor. The light source is a seven watt tungsten halogen lamp coupled by an optical fiber to the reactor. The reflected light is collected and coupled into a receiving multi-

mode fiber that has its output directed onto two silicon PIN photodiodes using a "hot mirror" that reflects light with wavelengths less than 700 nm onto one detector, and passes the remainder to the other detector. Two narrow wavelength ranges are selected from these high and low wavelength ranges using 10 nm bandpass interference filters centered at 550 nm and 900 nm. The light source is chopped with a simple rotating chopper wheel. This allows for easy recognition of the reflectance signal amid the ambient light due to the thermal emission from the susceptor, which is rotating between 1000 - 1200 rpm. Calculations used in Thermogrow are based on thin film interference of coherent monochromatic light. The wavelength of light generally used for growth-rate determination is 550 nm. Temperatures below 800 °C are extracted from the 900 nm light, and temperatures above 800 °C are extracted from the 500 nm light. In both cases, emissivity-correcting pyrometry is implemented by recording the DC thermal emission signal and using the fact that the emissivity is 1- reflectance. Information collected without emissivity correction is subject to artifacts that yield the data unusable. The Thermogrow program accounts and corrects for this and other artifacts and has been tested against SEM and XRD measurements to insure accuracy.

3.2 Cathodoluminescence, AFM, and TEM

Cathodoluminescence (CL), atomic force microscopy (AFM) and transmission electron microscopy (TEM) are three techniques that can be used to examine material quality and determine threading dislocation densities in both planar and cantilever epitaxy films. Each of these techniques has advantages and disadvantages in their ability to detect dislocations, the effort required to prep the samples and collect the data, and the

reliability of the data; therefore at least two of these techniques are used to draw final conclusions of the material quality and dislocation density.

Scanning cathodoluminescence (SCL) techniques are frequently used in the study of photonic semiconductors to assess the uniformity of minority carrier lifetimes and the presence of specific point, line, and planar defects [13]. SCL of GaN can be used to specifically quantify the threading dislocation density in both planar and selective area growth films [14, 15]. In these films threading dislocations appear as ~30 nm spots that have significantly reduced luminescence compared to the rest of the film. To implement this technique for dislocation observation, a JEOL JSM-IC845 SEM is equipped with a fiber optic light collector coupled to a photomultiplier/op-amp current/ voltage amplifier combination. The voltage output is processed by a Gatan analog to digital converter and image processor. The linearity of the light amplification system is crucial for quantitative sample-to-sample interpretation. The baseline measurements and detector position calibration are done with a phosphor standard to assure accurate measurements. Absolute beam current measurements are made with a Faraday cup/electrometer pair. Typical measurements are taken at 5 keV and 100pA with the gain adjusted to avoid saturation effects. The acceleration voltage, beam current, and gain set point are used in a normalization factor to accomplish wafer-to-wafer comparisons. This system can collect panchromatic images, or a filter can be used to eliminate wavelengths as desired.

SCL images are taken at different magnifications for different purposes. One of the strengths of CL is that it has the ability to scan over large areas. These large area scans have the ability to catch features that could affect devices that might not be caught by techniques such as TEM where smaller areas are typically sampled. Figure 8 shows a

panchromatic SCL image of a coalesced CE film. CL will image any dislocation that is electrically active. In this case in-plane dislocation loops, which will be discussed later, are easily observed and were not observed in AFM studies. These results were used to direct further TEM and AFM studies. Higher magnification images are used to measure dislocation densities.

In addition to panchromatic or monochromatic SCL images, CL spectral images can be taken to observe the wavelength components of the emission.

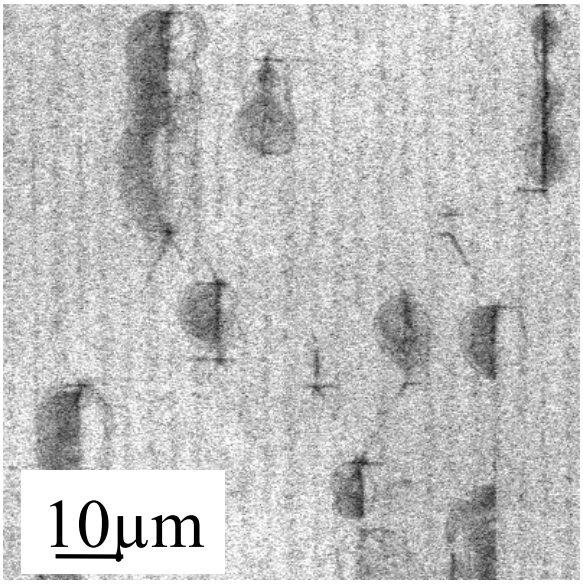

Figure 8. Panchromatic scanning cathodoluminescence image shows an area of 7310 μm^2. Both threading dislocations and in-plane dislocation loops can be observed with this technique.

TEM was used in both cross-section and plan-view orientations. Cross-section allows the behavior of threading dislocations emerging from the nucleation layer over the mesas to be examined, while plan-view examines larger surface areas and gives a statistically better value for the areal average dislocation density. The images were obtained with a Phillips CM20 instrument operating at 200 kV. A Gatan model 694

retractable slow-scan CCD camera was used to obtain digital images with 1024 x 1024 pixel resolution.

Cross-section specimens were prepared by gluing the GaN surface of a cantilever epitaxy specimen to a piece of sapphire, then gluing these into a stack of Si pieces approximately 4 mm wide by 4 mm high. The stack was turned on edge, and a 2.3 mm cylinder centered on the GaN layer was obtained by ultrasonic coring with BN abrasive. The cylinder was glued into a brass tube with 3 mm O.D. as required for a TEM specimen. Disks were sliced from the tube using a wire saw and were polished to ~100 μm thickness. A dimple grinder, Fischione Instruments model 2000, was used to mechanically polish the center of the disk to as thin as ~5 μm using 1 μm diamond abrasive slurry. The specimen was thinned to perforation in a Gatan model 691 PIPS ion mill using Ar ions accelerated to 3.5 kV and incident on the specimen at 4°. Cantilever material in the thin, tapered specimen around the perforation was imaged in the [1-100] orientation. Bright-field, dark-field and weak-beam diffraction conditions were used to image threading dislocations over the posts. Bright-field images obtained with **g** = (11-20) generally reveal the majority of the dislocations, but dark-field and weak-beam can provide further information. Weak-beam is useful for separating contrast from nearby dislocations if their density is high. When combined with **g** = (0002) images, the Burgers vector (**b**) and the type of the dislocations can be determined. Given that the dislocations are propagating vertically along the **c** direction as when no facet-based turning is used, individual dislocations can be classified as one of three types: **b** = **a** (edge), **b** = **c** (screw), and **b** = **a**+**c** (mixed).

Plan-view specimens were prepared by ultrasonically coring a 3 mm disk directly from the cantilever material, and dimple-thinning it from the back side, i.e., from the back of the sapphire substrate. The final thinning was done by milling with Ar ions incident from the back side only to preserve the original surface of the GaN for imaging. Dislocations were imaged in bright-field with **g** = (11-20); at the bright edge of a dark diffraction contour, the dislocations appear dark for counting.

AFM is performed using a Digital Instruments 3000 series controller in tapping mode. This technique can image the mixed threading dislocations and, under high-resolution conditions, the pure edge dislocations can be imaged as well. This technique is useful for looking at atomic level changes in the growth processes. Threading dislocations show up as small pits on the surface. The mixed dislocations are characterized by step pinning at the dislocations, and are the easiest dislocations to detect. Edge dislocations have a smaller pit than the mixed dislocations, and are not accompanied by step pinning. These edge dislocations can appear anywhere in the film, are often located mid-terrace and are sometimes grouped in lines. These dislocations are easily missed if the AFM conditions are even slightly less than optimal. Having a sharp AFM tip and making sure the system is free of noise caused by physical vibrations, electrical interference, and optical interference are imperative in detecting these dislocations.

Chapter 4: Cantilever Epitaxy

The basic growth procedure for cantilever epitaxy is to initially grow a nucleation layer followed by a series of high temperature growth steps between 950 °C and 1100 °C. These high temperature steps are a sequence that includes recovery from the nucleation layer, growth of a gable on top of the sapphire posts, and lateral growth to coalescence. Each of these steps is important in achieving a high quality planar surface with reduced dislocations and will be addressed separately in following sections.

4.1 Nucleation layer and growth of the gable

The first key step in cantilever epitaxy growth is the growth of the nucleation layer and the following steps to transition to smooth GaN growth on top of the posts. The growth starts out with an in-situ cleaning step at 1100 °C in pure hydrogen. This step has been shown to etch the sapphire surface and remove any hydrocarbons that remain from the processing of the substrates. It is followed by a nitridation step, which consists of NH_3 only, at a flow rate of 4500 sccm for 2 minutes at 250 °C. Although it is not entirely clear what happens during the nitridation step, it is thought that a thin AlN layer is formed or that the surface is hydrogen terminated. The nitridation step is followed by the growth of a low temperature nucleation layer. This can either be low temperature (LT) AlN or LT GaN, each of which has advantages and disadvantages for cantilever epitaxy that will become apparent. This layer is generally grown between 480 °C and 550 °C. The nucleation layer is followed by a series of high temperature growth steps, whose exact nature depends on the type of nucleation layer used. If a LT AlN nucleation layer

is used, then the transition from 3-D island growth to 2-D planar growth, called the GaN recovery stage, is as simple as growing at 1050 °C with a flow rate through the TMG bubbler of between 25 – 35 sccm and a flow rate of NH_3 of ~ 6000 sccm. The exact flow rates and conditions for GaN recovery are dependent on individual reactor geometries and nucleation layer thickness. In MOCVD of GaN, gallium is the limiting reactant in all cases. Nitrogen is present at anywhere between 600 and 3000 times the amount of gallium and a standard V/III ratio is ~1500. Because of this a V/III ratio of ~600 is called "nitrogen-starved". If a LT GaN nucleation layer is used recovery is performed under relatively nitrogen-starved conditions. This recovery is achieved through a series of steps that varies the V/III ratio from 600 to 1300 in a time incremented fashion. This NH_3-starved recovery is used because it gives the lowest dislocation densities in planar films. The theory is that if the film starts with fewer dislocations over the post then there are fewer dislocations to turn with subsequent steps. After the recovery, where the nucleation grains have coalesced into a nearly planar film, the specialized steps required for cantilever epitaxy can begin. The recovered film is polycrystalline, with grains that can be as large as 5-10 μm in width. To date, only vary small amounts of single crystal, bulk GaN have been produced.

As was seen in the earliest cantilever epitaxy work and in Facet Controlled ELO (FACELO) research [9, 16, 17] VTDs turn and run horizontally when they encounter a free faceted face. This can be seen in ELO pyramids and near the edges of large cantilever posts. In order to investigate this phenomenon for cantilever epitaxy two experiments were performed. Both experiments used standard cantilever epitaxy substrates as described earlier in this document, and used an AlN nucleation layer

deposited at 480 °C. This was followed by growth at 1050 ° C for a planar growth thickness of 0.6 μm for the first sample and a growth for 0.1 μm at 1050 °C and 0.5 μm at 950 °C for the same planar growth thickness for the second sample. These growth conditions were selected based on previous GaN kinetics studies in the ELO system. An educated guess could be made as to what growth conditions would be needed to give the desired feature. The decision to grow for the same growth thickness, instead of a set growth time, was made in order to try to minimize any run-to-run variability in the growth rate. The planar growth rate was calculated using in-situ reflectance monitoring. The evolution of the facets was then examined by SEM. Figure 9a and b illustrate the two cases.

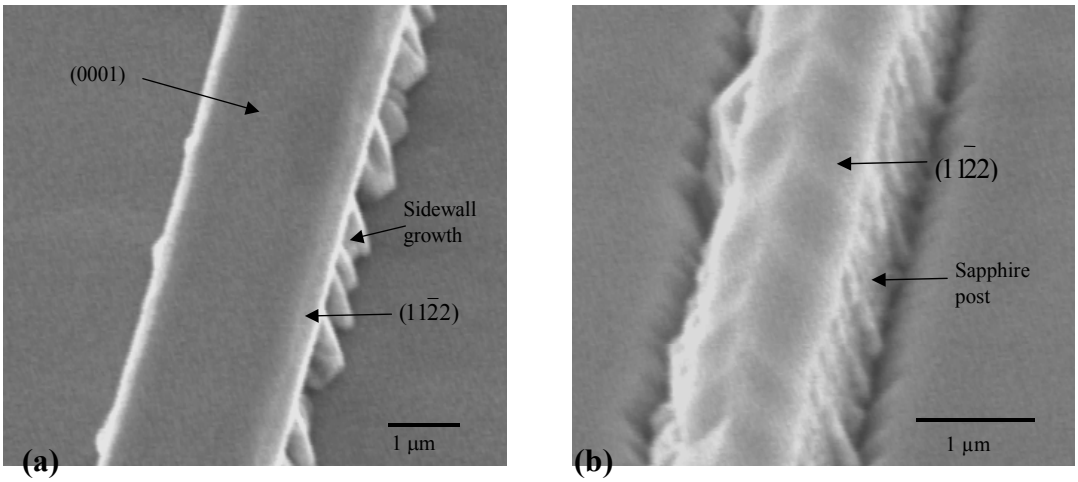

Figure 9 (a) SEM of growth at 1050 °C growth step for 0.6 μm on top of sapphire post. A small amount of faceting is seen at the edge; (b) shows a SEM of the similar growth at 950 °C to force a faceted gable.

The result of the 950 °C growth step was to force a gable to form on top of the post. This is the ideal condition for turning vertical threading dislocations to the horizontal direction. This experiment was then repeated but growth was continued at 1100 °C until adjacent cantilevers coalesced. These samples were then grown to a total

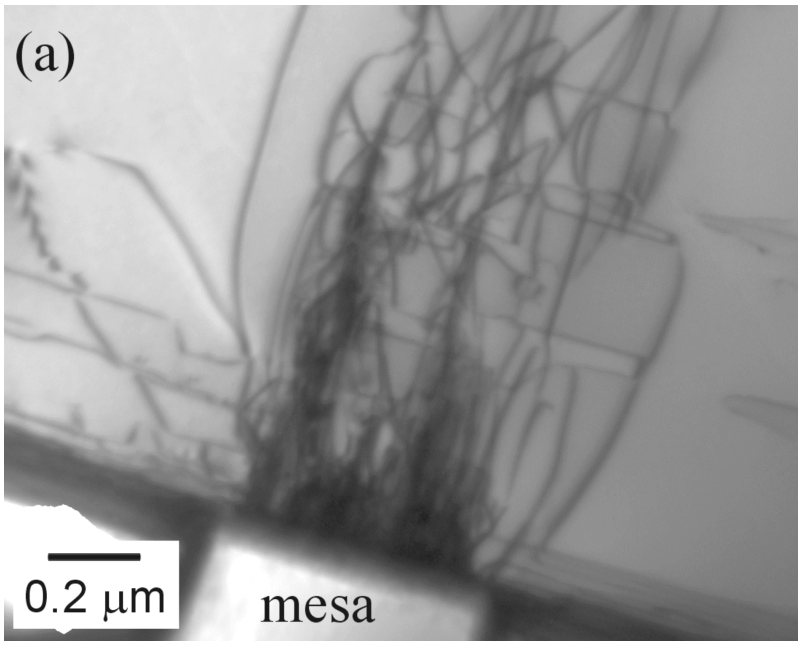

Figure 10. $(11\bar{2}0)$ bright-field XTEM image of VTDs over a 0.54 μm wide mesa with no faceting as shown in Figure 9a.

thickness of 4 μm. Cross-sectional transmission electron microscopy (XTEM) images obtained from the specimen without facets show that ~ 30-70% of the threading dislocations are turned horizontal, as seen in Figure 10. This unforced turning is attributed to several factors. In Figure 9a, a small amount of faceting is seen at the edge of the GaN during the 1050°C growth. These are smaller versions of the $(11\bar{2}2)$ facets seen clearly in Figure 9b. Image forces on the dislocations may attract them laterally to the vertical free surface of the GaN sidewall and turn them when the growth condition is changed. In addition, some dislocations annihilate each other by forming loops. This sidewall-dominated turning mechanism is greatly enhanced in the sample with faceting.

The number of dislocations that are ultimately turned by this faceting method is dependant on the post width. Figure 11 shows a post that is 0.65 μm wide. In this example all of the 26 initial dislocations were turned using this faceting method. Figure 12 shows a post that is 0.91 μm wide. Two of the 53 initial threading dislocations

propagate to the surface. The variation in the post width occurs during the fabrication of the cantilever epitaxy substrates. For wider posts the gables do not come to a complete point, i.e., some basal plane remains. This has been routinely observed with SEM and can be geometrically calculated, as the angle of the $(11\bar{2}2)$ facet grows at 58.4 ° with respect to the substrate. Future experiments could increase the growth time, adjust the temperature, or adjust the V/III ratio of the faceting step to accommodate varying post widths. In addition, processing advancements are being made to increase the overall wafer uniformity. The key is to form a fully pointed gable before the lateral growth step proceeds. As seen in Figure 11 it is possible to turn all of the dislocations if the conditions are right, both major types of dislocations edge (**b=a**) and mixed (**b=a+c**) can be redirected effectively by the facets.

The CE research started with LT AlN nucleation layer (NL) because programmatic priorities were to develop high electron mobility transistors (HEMTs) on sapphire cantilever epitaxy substrates and LT AlN nucleation layers were thought to be more insulating than LT GaN nucleation layers. This nucleation layer deposits on all surfaces of the etched sapphire substrate and causes GaN nucleation both on the top of the sapphire posts and the sidewalls as seen in Figure 9a. This sidewall growth was found to be problematic for future stages of the growth as it interferes with the lateral progression of the cantilevers. To solve the issue of growth from the sidewalls of the cantilever the nucleation layer was switched to a LT GaN nucleation layer. This nucleation layer is more common for planar GaN on sapphire and it typically produces higher quality GaN with fewer threading dislocations. In most cases it does not cause growth from the sidewalls of the sapphire posts.

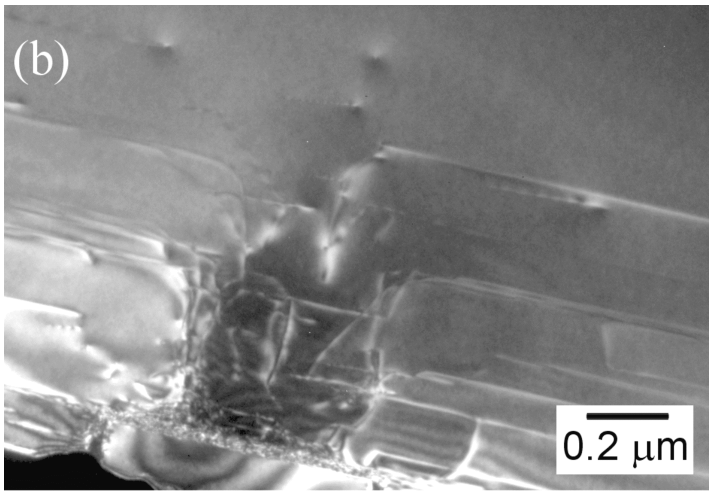

Figure 11 shows dislocation turning for a sample with forced faceting where the mesa width is 0.65 μm wide. In this TEM none of the 26 dislocations reach the surface.

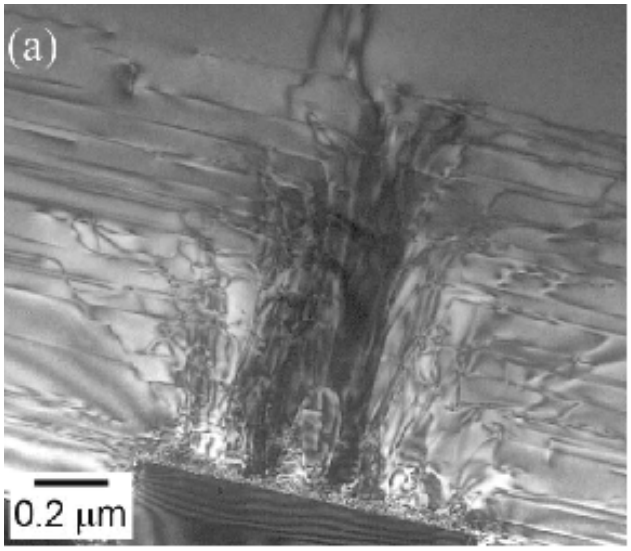

Figure 12. $(11\bar{2}0)$ dark-field XTEM images of VTDs over a 0.91 μm wide mesa. Two of the 53 original VTDs thread to the surface.

In order to get high quality GaN growth on sapphire this nucleation layer has to be thick enough to produce a sufficient number of GaN nucleation sites, which can then coalesce to a planar film. Typically for planar growth the thickness of this nucleation layer is controlled by in-situ reflectance monitoring. The reflectance signal is normalized to the reflectance of sapphire at room temperature. This removes any variation due to

ambient changes in the reflectance signal. The nucleation layer is grown until the reflectance level reaches 0.21 (arbitrary units) for single side polished wafers and 0.13 for double side polished wafers, which is ~ 30nm for each case. This is then followed by an annealing step in H_2 and NH_3, which is observed to create larger grains. During this period the reflectance drops to below that of the original sapphire due to NL decomposition and creation of larger GaN grains. Tracking the reflectance signature of the growth run allows run-to-run comparison of layers, which are subsequently buried.

One difficulty with the cantilever epitaxy growth using the LT GaN nucleation layer is that the width of the post tops affects the density of the nucleated grains on the post top. This was not a problem when a LT AlN nucleation layer was used.

It is difficult to examine the quality of the nucleation layer by itself so in order to investigate changes to the nucleation layer growth conditions the nucleation layer is followed with 10 minutes of growth at 1050 °C and 15 minutes at 950 °C. GaN planar growth is typically done ~1050 °C and this step is needed to help form a 2-D growth surface on the top of the post. 950 °C is significantly outside the temperature range for high quality planar growth and although this temperature is useful for forming a gable on top of the post, the growth needs some growth at higher temperature in order to recover from the nucleation layer stage. Combining these two steps gives enough GaN to easily examine the wafers with a SEM, and simulates the gable-forming step that is needed for threading dislocation turning. As will be shown later the uniformity of the gable, shown in Figure 14, is critical to the future cantilever steps. Changes in the quality and completeness of the gable on top of the post are monitored as a marker for changes made to the nucleation layer.

Using the above technique it is determined that using a 500 °C nucleation layer produces a high quality complete gable. Figure 13 shows an example of a nucleation layer grown at 550°C. This nucleation layer yields sparse growth on top of the sapphire posts and significant amounts of growth in the trench. Growth in the trench is indicative of the growth on a planar unetched surface. Figure 14 shows an example of a gable that can be grown with a nucleation layer grown at 500 °C. Further reduction of the nucleation layer temperature leads to growth on the sidewalls of the sapphire posts and other undesirable behavior such as polycrystalline GaN. Various other changes in the growth conditions were attempted which include, but are not limited to, changes in the growth time, V/III ratio, the annealing time and temperature, and the pre-treatment of the wafer both ex-situ and in-situ before growth. The only variable that made a significant difference was the temperature of the nucleation layer.

Just as a change from a large area planar substrate to a post affects the nucleation layer, so does a change from a 1 μm post width to a 0.5 μm post width. These types of variations can be common over a 2-inch substrate and the ultimate solution would be to have completely uniform processing. Processing a 2-inch substrate with a uniformity in the post width is difficult, so growth conditions are selected for the mean post width on the wafer.

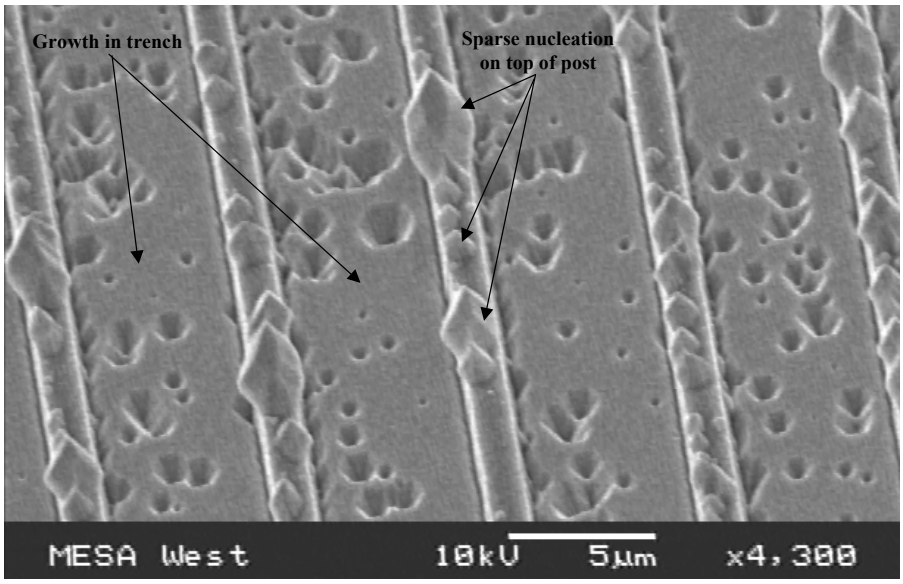

Figure 13. Example of nucleation layer at 550°C. Sparse GaN islands are present on top of the sapphire posts, while the GaN growth in the trench is significantly more complete.

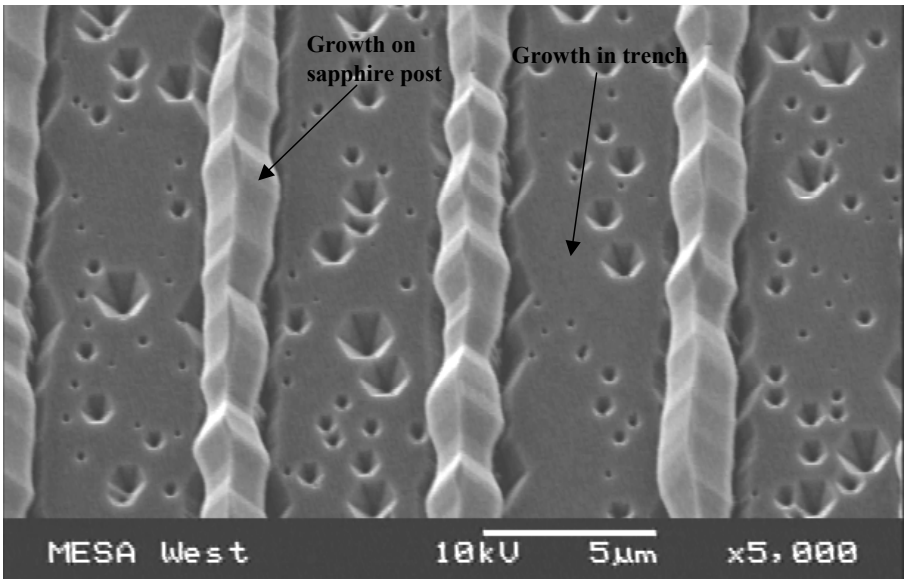

Figure 14. Example of nucleation layer grown at 500°C. Nucleation on sapphire post is much more complete which yields a more uniform faceted gable.

One solution, in theory, is to make the post widths significantly wide so that nucleation on the top of the post is not an issue, but there is another trade-off that was

eluded to earlier. As the post tops get wider, it requires more growth time at the 950 °C faceting step to have a completely pointed gable (with no basal plane). At the current time trenches can be made with a depth of ~2.5 μm. This trench depth must accommodate the growth needed to form a complete gable, without a basal plane at the top, and the time it takes to coalesce the cantilevers, without filling up the trench to the point where the GaN interferes with the overgrowing cantilevers. Because of this, the post widths cannot get wider unless the trench depths can get deeper.

4.2 Lateral overgrowth of cantilevers

Once the gable is formed at 950 °C the growth temperature is increased to laterally overgrow the cantilevers. Standard growth conditions are to start the lateral growth at 1080 °C for 4500 sec and then proceed with growth at 1050 °C for an additional 3600 – 4200 sec. At these higher temperatures the growth rate of the $(11\bar{2}2)$ and $(11\bar{2}0)$ facets increase with respect to the basal plane. An average lateral to vertical growth rate ratio is ~ 3. The relative growth rates change as the coalescing cantilevers approach each other. This phenomenon is discussed in detail later in this section. Figure 15 shows a cross-section SEM of an overgrown cantilever before coalescence. This picture also demonstrates the delicate balance between the growth time needed to grow a complete gable and the growth time needed to overgrow the trench before the GaN filling in the trench interferes with the laterally growing GaN. Several factors make this task more difficult. Even when GaN has difficulty nucleating on the top of the post, GaN readily nucleates in the etched cantilever trench as shown in Figure 13 and Figure 14. It is known that plasma etching, which predominately occurs by

sputtering, causes significant damage and potentially increases the number of nucleation sites. So in cases where less nucleation occurs on the post top, the trench GaN may already be fully nucleated. In addition, conditions that enhance the basal plane growth, such as growth at 950°C also enhance the growth in the trench. This means that the time spent on vertical growth steps is limited unless processing advances are made to achieve deeper trenches.

During these lateral growth steps the only in-situ growth rate measurement is on the center monitoring section, which is a measure of the basal plane growth rate. Because of this growth runs have been stopped after the initial lateral growth step at 1080 °C to measure the lateral growth rate. The lateral growth rate at 1080 °C changes both from run to run (due to unintentional temperature or local V/III changes in the reactor) and as the overgrowing cantilevers start to approach each other.

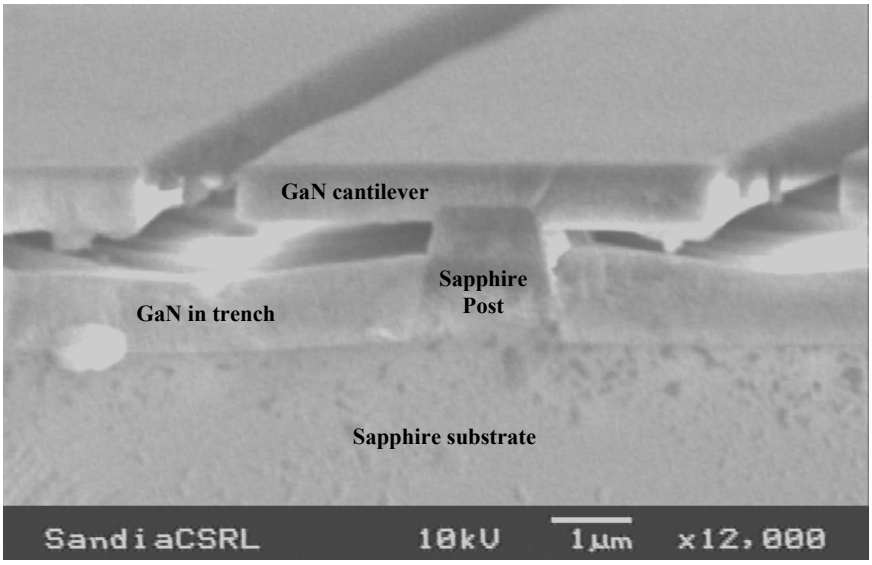

Figure 15. Cross-section SEM of laterally overgrown cantilevers before coalescence. The rectangular shape is indicitave of growth above 1080°C.

As a result, a lateral growth rate of 3.3 μm/hr measured after 1800 sec of growth at 1080 °C cannot necessarily be used to predict the total time needed to coalesce the film, even if the growth conditions stayed the same. Figure 16 shows several lateral growth measurements from different runs that illustrate this point. If the lateral growth rate had stayed constant the lateral span of the cantilever at 3600 sec would be ~3.3 μm, as indicated by the solid line, instead of ~2.3 microns as the data shows. As the cantilever growth proceeds in time, the lateral growth rate slows down. This change in growth rate is greater than what could be accounted for due to unintentional temperature changes, such as drift in the thermocouple. The change in the lateral growth rate as the cantilevers approach coalescence is something that cannot be explained with current GaN ELO kinetic models and will be addressed in the future work section. In addition it is not believed that the proximity of the approaching cantilevers affects the concentration gradient at the surface, and thus the growth rate; the total exposed growth surface area does not change significantly over the whole growth process. Consequently the change in growth rate is not due to a gas-phase diffusion limitation. The fact that there are two types of variation in the lateral growth rate, day-to-day changes in the reactor and a change as the fronts approach each other, makes it very difficult to predict when the cantilevers are going to coalesce. The following sections will discuss the desire to control the growth so that the cantilevers are partially overgrown at high temperature, followed by a lower growth temperature to bring the cantilevers together with $(11\bar{2}2)$ facets rather than $(11\bar{2}0)$ facets. This may prove extremely difficult if the factors influencing the lateral growth are not better understood.

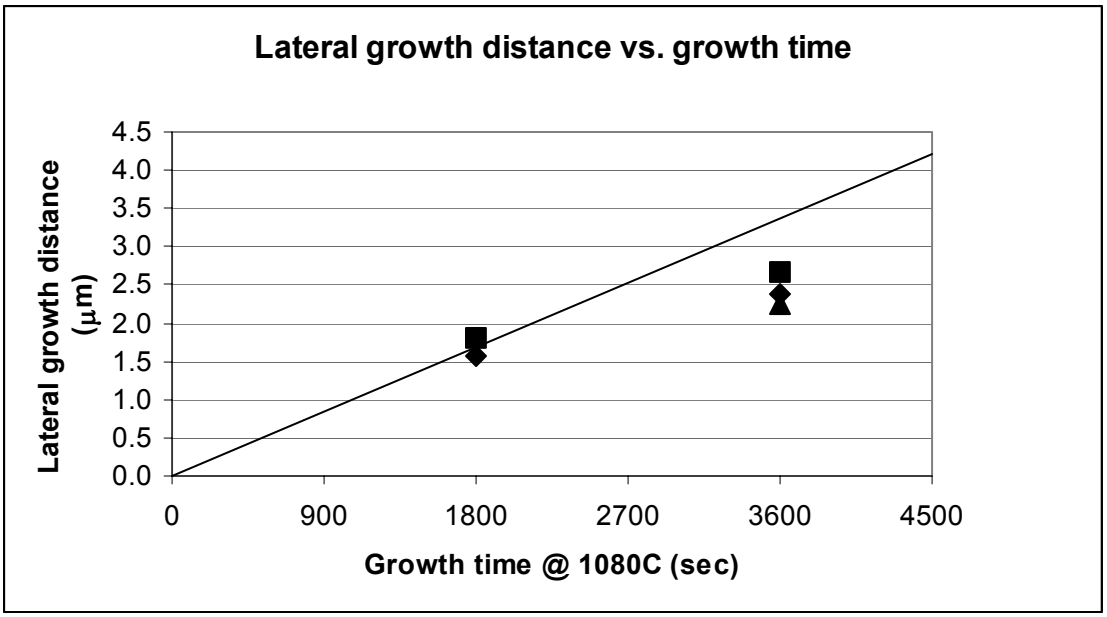

Figure 16. Graph of the lateral growth span of a cantilever, measured from the edge of the post, with respect to growth time at 1080 °C. The solid line indicates the trend that should have been followed if the growth rate remained constant from 1800 seconds onward.

4.3 Coalescence of cantilevers and resultant planar film

As discussed in the previous sections, a lot occurs before the cantilevers get to the point where they have to stitch themselves together. In the ideal case, two adjacent cantilevers would be in perfect alignment and the merging would happen without the formation of any additional dislocations. In reality, the merging of two cantilevers can be very problematic. There are five methods used to study the quality of a coalesced cantilever epitaxy film. These include, optical microscopy, SEM, AFM, CL, and TEM. The techniques can provide unique and complementary data when trying to qualify the process.

4.3.1 Interference from the GaN growing in the trench

The first step in determining whether a wafer is viable cantilever epitaxy substrate is to determine whether all of the growth steps were completed without the GaN growing

in the trench interfering with the laterally growing cantilevers. Using optical microscopy gives is an easy way to determine whether this has happened. This is important to monitor because trench GaN can interfere with the lateral overgrowth to generate threading dislocations. Figure 17 shows an example of an optical micrograph where the sapphire posts, coalescence fronts, and interference from the GaN in the trench can easily be identified. Essentially, any feature that shows up as a dark object is one where there is not a gap between the top of the film and the substrate. The only index of refraction difference is at the surface between the epitaxy and air. The areas that appear as a lighter color are a result of an index of refraction change not only at the surface, but also between the cantilever and the air gap. This difference makes it possible to distinguish between films that still have a gap between the trench and the bottom of the cantilevers.

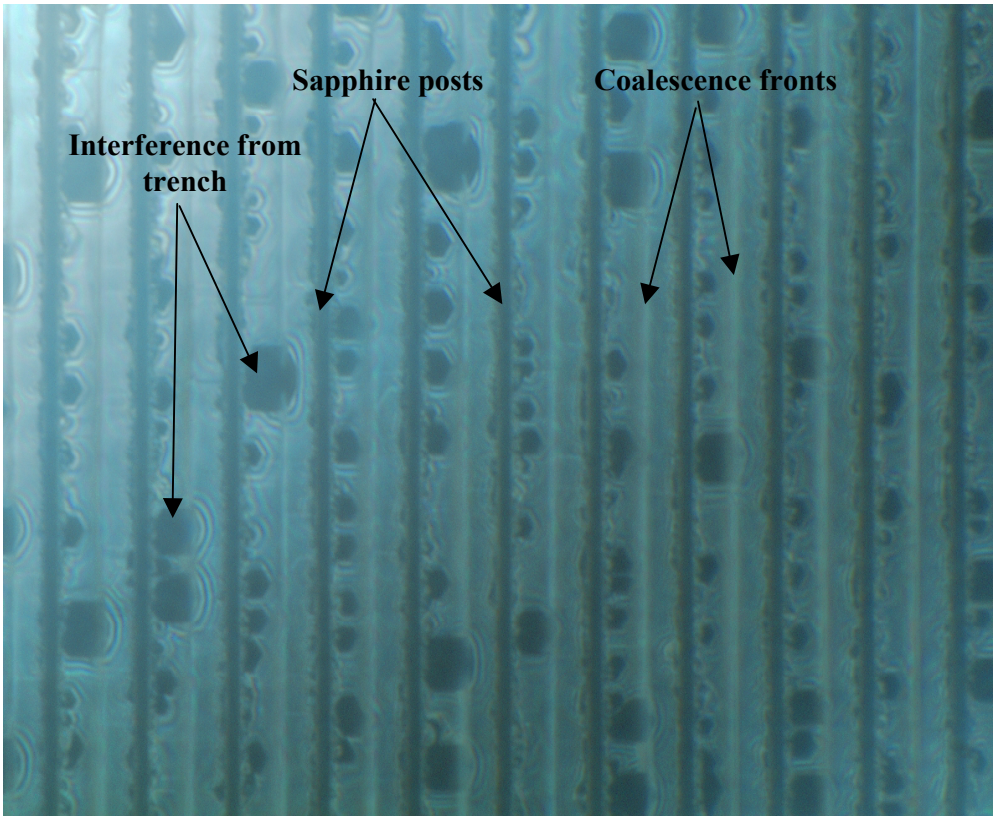

Figure 17. Optical micrograph of a coalesced cantilever epitaxy film where the sapphire posts, coalescence fronts and interference from the GaN in the trench can be identified.

4.3.2 Coalesced film surface discontinuities and dark-block defects

Optical micrographs taken to determine if the trench growth has interfered with CE GaN are done with the microscope focal point on the top of the sapphire post. An alternative focus point is on the top of the film. This is the first way to determine if everything has gone well with the coalescence and if the films have completely coalesced. Figure 18 shows an example of features, as examined by optical micrography, that appear when the fronts coalesce in a non-ideal fashion. These discontinuities can also easily be seen in the SEM and correlate with large in-plane non-radiative defects, denoted as "dark-block" defects, seen in panchromatic CL scans. Figure 19 shows an example of these surface discontinuities as they relate to CL images. The features seen in

SEM images directly correlate to dark-block defects in CL. These features have several signatures, and have been examined in detail by SEM, AFM, and TEM. Figure 20 shows a cross-sectional SEM image taken of a representative surface feature. This image shows that the discontinuities are not purely surface features. These discontinuities occur when two cantilevers come together misaligned from each other. There is always a height difference between the two joining cantilevers, sometimes as much as 200 nm. In addition, there is a gap between the two cantilevers that extends the entire height of the cantilever. This is seen in cross-section TEM as well as with the SEM. The cantilevers often appear as if one side is overgrowing the other, pinned at the end of the crack. The overgrowth can often extend 10-15 μm laterally on the surface as seen in the optical micrograph in Figure 18. Plan-view TEM studies around these dark-block defects and their correlating surface discontinuities show that these blocks are made up of lateral dislocation arrays bowing outward from a surface discontinuity. These dislocations often bow laterally as far as the next coalescence front and can sometimes include multiple posts and coalescence fronts.

These dark-block defects have been seen in films with both LT AlN and LT GaN nucleation layers as long as the low temperature step intended to turn dislocations was present.

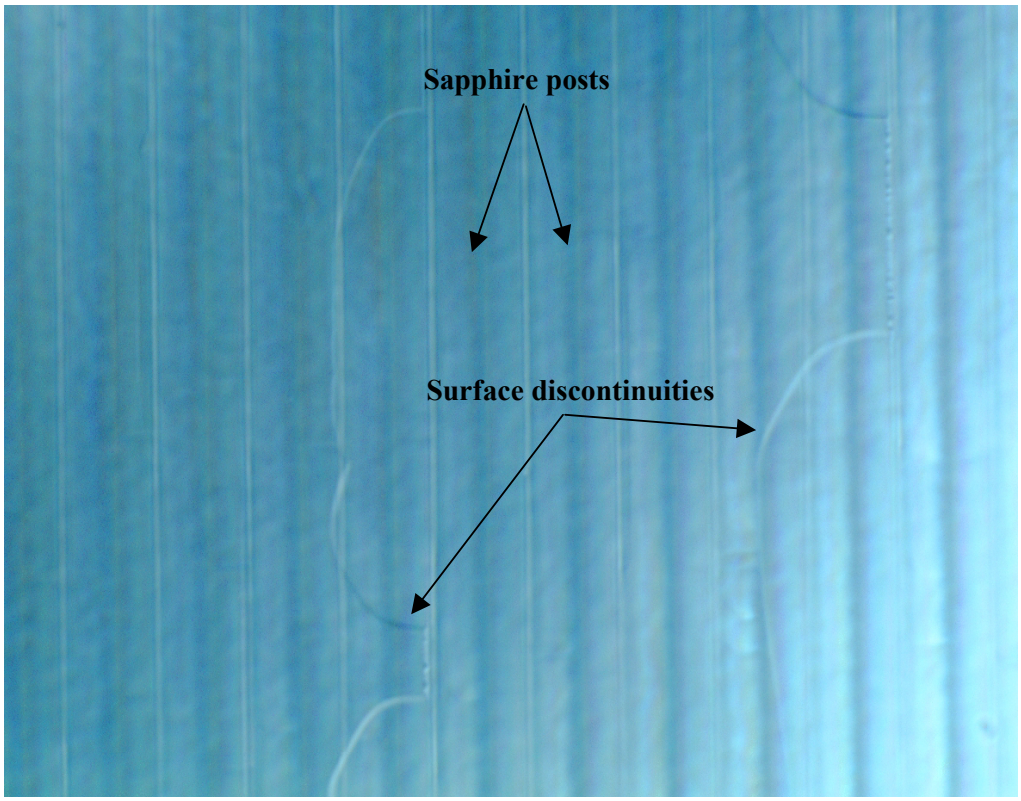

Figure 18. Optical micrograph of surface discontinuities present after coalescence of cantilever structures.

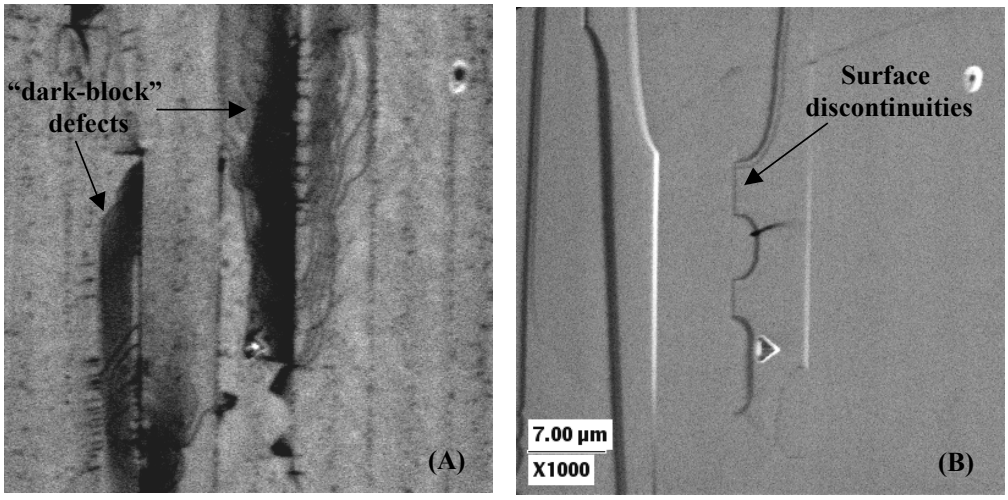

Figure 19. (A) Scanning panchromatic CL and (B) secondary electron (SE) micrographs of a coalesced cantilever substrate where surface discontinuities are present. These surface discontinuities seen in the SE images directly correlate with the "dark-block" defects seen in the cathodoluminesce scan.

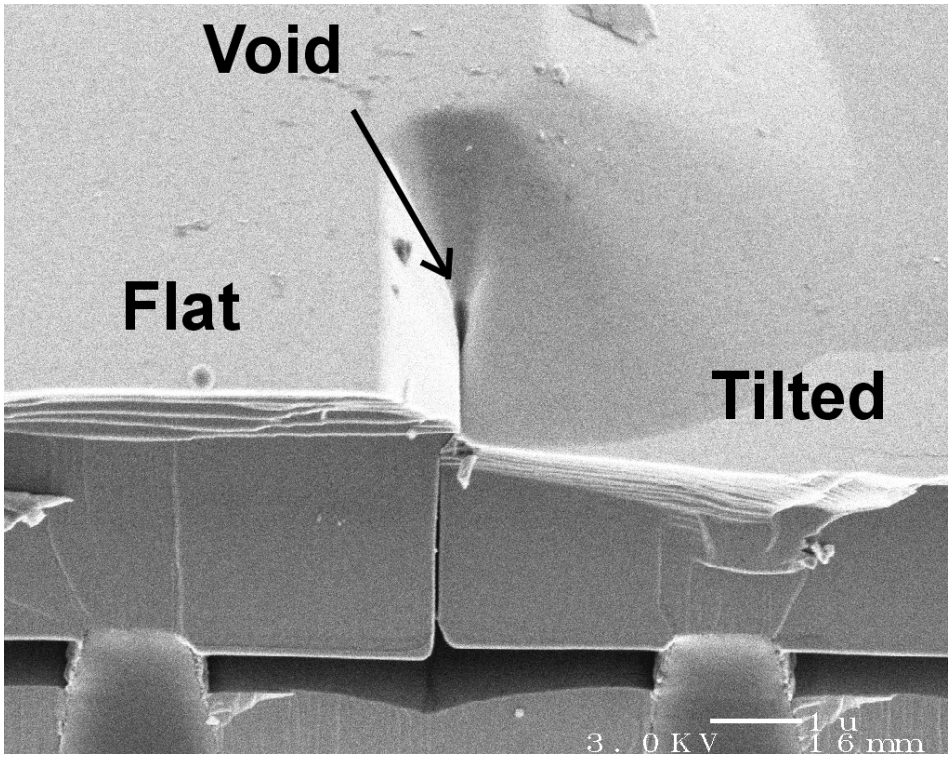

Figure 20. Cross-sectional SEM of a surface discontinuity at the intersection of two cantilever wings.

Fortunately, several samples, CV3004, CV3006, and CV3008, have been grown where dislocation turning was used and no dark-block defects or surface discontinuities are present. Figure 21a shows representative panchromatic CL images of CV3004, clearly coalesced without dark-block defects. Several areas over each of the three wafers were imaged to verify that this was not an isolated effect.

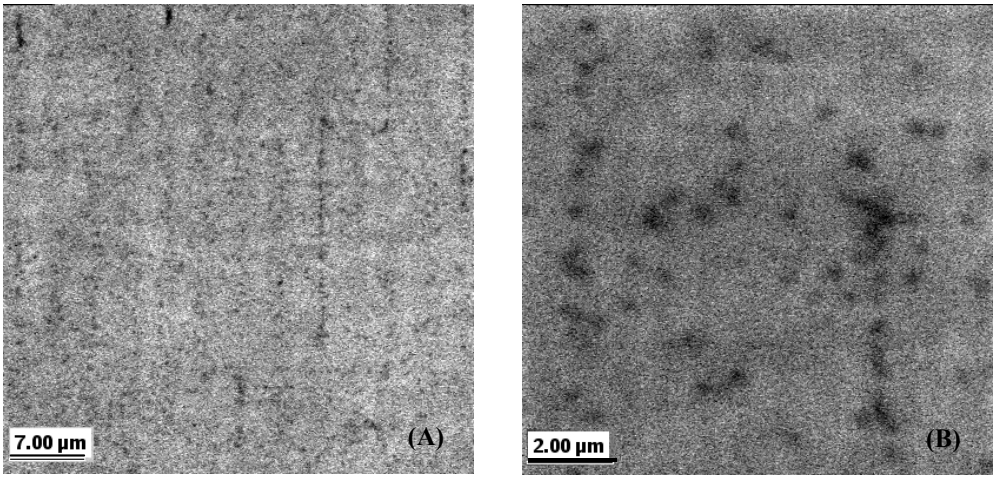

Figure 21. Panchromatic CL images of coalesced CE films without dark-block defects and surface discontunities.

4.3.3 Effects of silicon doping on dark-block defect formation

Wafers CV3004, CV3006, and CV3008 were grown under nominally the same conditions as many other samples previously grown. The only noticeable difference in the growth set points between this sample and others was that these three samples did not have any intentional silicon doping (GaN is generally unintentionally doped n-type). Most earlier growths had intentional Si doping (GaN:Si) with a doping level of 5E18 cm^{-3}. This was done in an attempt to make the bottom cantilever epitaxy layers for LED growths. For reasons having nothing to do with the cantilever epitaxy evolution, the decision was made to grow the cantilever layers without intentional doping. The result, as shown by CL in Figure 21, was films that had substantially fewer dark-block defects. Upon reviewing all of the cantilever runs specifically looking for a connection to silicon doping, there is a qualitative correlation between the size and number of the dark-block defects and the intended level of doping. To test if Si doping is related to the undesirable features and to look at the difference between doped and un-doped runs at each stage of

growth (gable, laterally grown but uncoalesced cantilevers, and coalesced films) a series of growths was performed, stopping to examine each step with SEM. These experiments showed that the lack of Si doping was not the only factor involved in successful cantilever epitaxy growth. However, wafers with dark-block defects and surface discontinuities can be grown even without Si doping. The fact that the successful experiments were not immediately reproducible without silicon doping does not mean that it is not one of many contributing factors. Because of this, and because of the fairly strong trend relating the number and size of dark-block defects to silicon doping, silicon doping was eliminated for the remainder of the experiments while trying to figure out the causal relation to dark-block defects.

The rest of the growth conditions set points (such as temperature, gas flow rates, and pressure) were the same as many other runs. This means that a full understanding of the scope and magnitude of conditions that affect the cantilever evolution and quality has not yet been achieved. From this point on, the analysis consists of the attempt to understand each step that leads to these successful growths and try to repeat them.

4.3.4 Effect of substrate quality

After examining the growth condition set points for differences, the next step was to review the substrate conditions. As was mentioned earlier, a great deal of time is taken to characterize each substrate prior to growth, so that when a problem arises with the growth the substrate can be ruled out as a cause. The width of the post top and the depth of the trench have a significant effect on the growth results, so the pre-growth measurements were reviewed. The substrates used for CV3004, CV3006, and CV3008 were not significantly different than other substrates used throughout the project. The

post widths ranged from 0.8 μm to 1.25 μm and the depth averaged 2.5 μm for all of the samples. This is well within the normal range for wafers.

4.3.5 Effects of cantilever morphology just before coalescence

The third step in examining these wafers was to look for differences in the cantilever evolution and coalescence behavior. CV3004, CV3006, and CV3008 were all grown with a recipe that in the past had produced fully coalesced wafers with dark-block defects, except for the lack of intentional silicon doping. These three wafers were grown for 4500 sec at 1080 °C and 4200 sec at 1050 °C. Based on these growth times the wafers were expected to fully coalesce. Previous wafers had coalesced with just 3600 sec of growths at both temperature steps. The extra time was added to try to compensate for any growth rate change due to a possible 10-20° difference from the set point. As was mentioned earlier in section 4.2 the lateral growth rate not only varies because of temperature variation from the set point, but also as the cantilevers approach each other. Instead, an examination of CV3004, CV3006, and CV3008 by optical microscope and SEM showed that they were not fully coalesced and that they had prominent $(11\bar{2}2)$ facets showing. The cantilevers had coalesced in some areas but had gaps in other areas. This lack of coalescence was radially dependant and the features toward the edge of the wafer were not coalesced at all. This is an important difference from other samples which coalesced with $(11\bar{2}0)$ facets and in only an hour of growth at 1080 °C. AFMs of coalesced regions at the center of the wafers show interesting features. Figure 22 shows an example of a surface feature that closely resembles a smaller version of the surface discontinuities seen in Figure 18 and Figure 19b. These smaller features were not noticeable with either an optical microscope or the SEM. The height of this feature and

similar ones ranged from 10 nm to 40 nm. In order to coalesce the outer portions of the sample, a regrowth was completed for 1 hr at 1050 °C. After this growth these small surface features were no longer apparent by AFM.

In addition to CV3004, CV3006, and CV3008, which were grown without dark-block defects mentioned previously, a fourth successful wafer (GNC0681A) coalesced without surface discontinuities or dark-block defects. These four wafers had the same growth conditions up to the 1080 °C growth step. At this point GNC0681A grew for 3600 sec at 1080 °C and 3600 sec at 1050 °C. As with the CV3000 series this wafer did not coalesce as expected. At this point the $(11\bar{2}2)$ faceting was enhanced by growing at

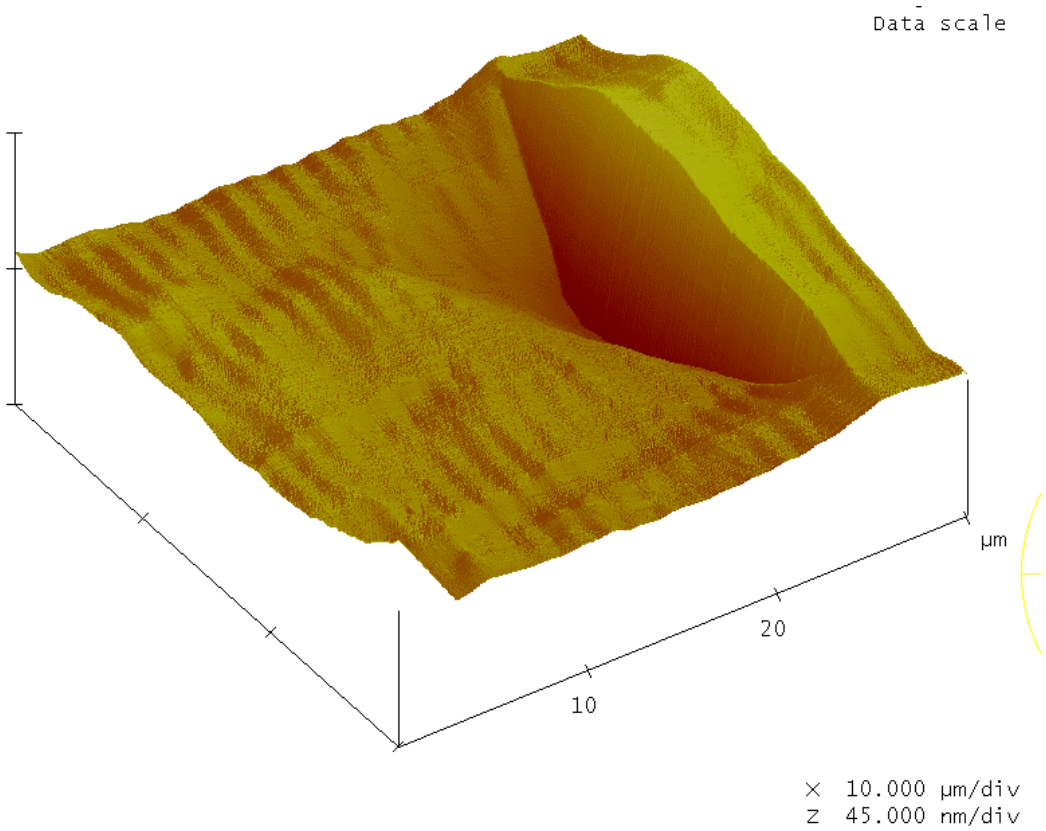

Figure 22. AFM image of surface discontinuity on CV3006. Similar features were seen on CV3004 and CV3008. These features disappeared after a regrowth at 1050 °C for 1 hour.

500 torr. This pressure is high compared to the normal growth pressure of 140 torr. Growth at high pressure acts in much the same way as growth at low temperature and GaN tries to grow to a gable. This growth gave a partially coalesced film and regions that were not coalesced had very noticeable $(11\bar{2}2)$ facets. Figure 23 shows SEMs at different magnifications, which clearly illustrate that the high-pressure growth resulted in prominent $(11\bar{2}2)$ facets. SEMs of CV3006 had almost identical surface features in the form of $(11\bar{2}2)$ faceted gaps between regions of coalesced cantilevers.

This growth was followed by a growth at high temperature and lower pressure (150 torr) to fill in the trenches and planarize the surface. The result was a beautifully coalesced film that did not have surface discontunities or dark-block defects.

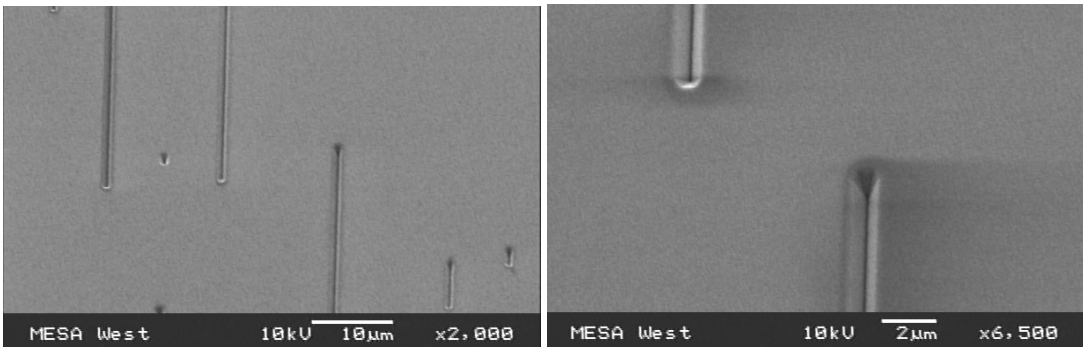

Figure 23. SE micrographs of the partially coalesced substrate after 500 torr growth. These trenches are similar in size and frequency to features seen in CV3004, CV3006, and CV3008.

4.3.6 $(1\bar{1}01)$ *steps on cantilevers proceeding coalescence*

Although the data now indicates the importance of the $(11\bar{2}2)$ facet, as it relates to eliminating dark-block defects, prior to coalescence, this cannot be the entire story. Many runs before the CV3000 series show that the lateral growth of the cantilevers is greatly affected by the condition of the gable that proceeds it. Figure 24 shows as series

of four SEMs. (A) and (B) were taken after the growth at 950°C. This was a portion of the wafer where there was noticeable radial variation of the quality of the gable. This difference from center to edge is attributed to a difference in the growth conditions at the surface. The exact nature, most likely a temperature variation, is still under investigation. The important thing to notice, however, is that the variation in height along the wafer is significantly different for (A) and (B). In area (A) the gable is complete and no sapphire substrate can be seen. As you look along the posts you see striations on what you would expect to be a smooth $(11\bar{2}2)$ face. In actuality the faces that are appearing are $(1\bar{1}01)$ faces in conjunction with smaller $(11\bar{2}2)$ faces. The $(1\bar{1}01)$ faces are the slowest growing faces in the GaN system and they appear readily at low growth temperatures. Many samples show ruminants of these steps after coalescence and they are often associated with the surface discontinuities and dark-block defects.

The angle of the $(11\bar{2}2)$ facet and $(1\bar{1}01)$ facet are 58.41° and 61.96° respectively with respect to the surface. Taking SEMs that look directly down on the top of the posts allow for the measurement of the width of these facets from which a height can be calculated. The approximate height variation along the gable top in (A) is 0.1 μm while the height difference for (B) can easily be 0.5 μm. This non-uniformity along the gable leads to the features seen in (C) and (D). These features are $(1\bar{1}01)$ faces that are running perpendicular to the desired lateral growth direction and are most likely a result of the height variance along the gable.

Low magnification SEMs give counts of the steps in each area. There were $3x10^4$ steps/cm^2 for area (A) and $4x10^5$ steps/cm^2 for area (B). It is easily seen that the quality

of the lateral growth of the cantilevers is directly related to the quality of the gable. In addition the steps in (B) seem to be taller than the steps in (A), although this was not quantified. These steps have been examined by AFM and are generally on the order of 100-200 nm tall. They do not always form an abrupt step. Sometimes they are composed of a series of facets that make a continuous smooth transition from the bottom to the top level. In addition, the steps are often seen in pairs, where a step that runs from high to low is followed closely by a step that runs from low to high. These pairings can be as close as a micron apart but can have also been routinely seen to be 10s of microns apart. The data suggests that if cantilevers can be created without these steps a coalesced film without dark-block defects can be formed.

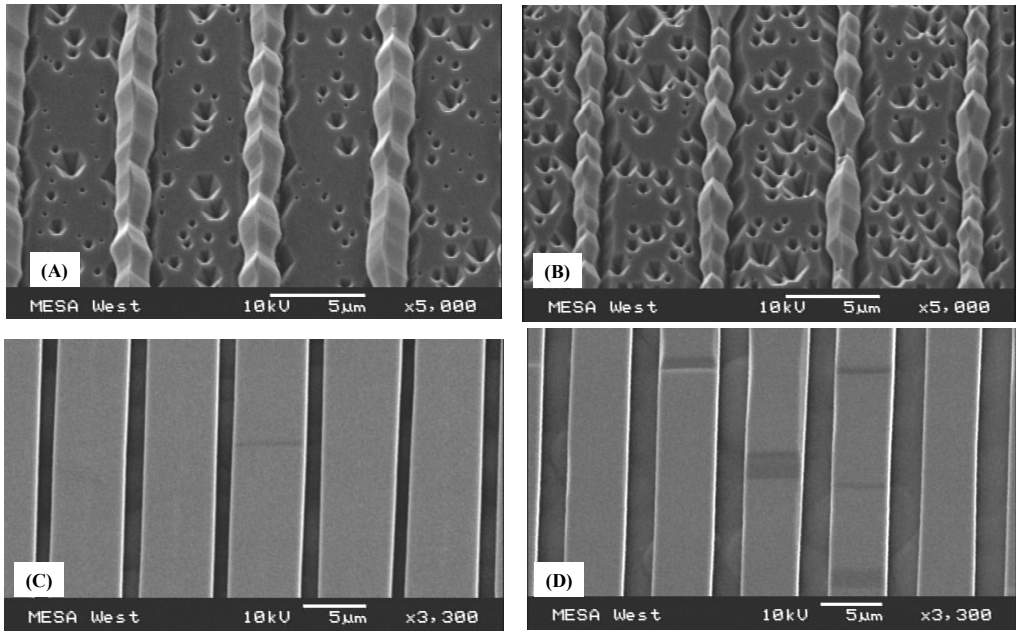

Figure 24. SEMs taken at the perspective of 30°. (A) shows a gable that is fully coalesced without a lot of variation along its length. (B) shows a gable that is less developed than (A). (C) shows the same area of the wafer as (A) after the wafer had been grown on for 1 hour at 1080°C. (D) shows the same area of the wafer as (B) after 1 hour of growth at 1080°C.

It seems logical that the best thing to do would be to not create these steps in the first place and therefore remove the need to get rid of them. It is known that the presence of these steps is always associated with dark-block defects in the coalesced film. However, after many growths it seems that the only conditions that do not produce steps are to have a completely uniform gable or to not grow the gable in the first place.

Creating a highly uniform gable could be accomplished using a LT AlN nucleation layer which gives even growth of the gable, but for reasons discussed earlier this is not a viable option. In addition, a wafer with a LT AlN layer was stopped before coalescence to look at the condition of the cantilevers. This sample did not have any steps along the cantilevers yet it had numerous dark-block defects. This data shows that

it is not only the quality of the cantilevers that matters, but also the conditions under which they coalesce.

One analysis technique would be to monitor the crystallographic tilt of the cantilever wings as it relates to the quantity and size of these steps. Crystallographic tilt has been successfully measured for ELO substrates and the tilt in the overgrown ELO wings shows up as symmetric peaks on either side of a center peak which is the layer of GaN underneath the dielectric mask [18, 19]. Wing tilt of over 0.2° is associated with poor coalescence and the creation of dislocations at the coalescence fronts. Initial studies did not show any significant wing tilt for uncoalesced wings on cantilever epitaxy substrates and the results were difficult to interpret because CE does not have a thick GaN base layer to reference the shoulder peaks from, as is commonly done with ELO films, to. The analysis of these results gave a null result and for that reason, XRD has not been routinely used as an analysis technique for these experiments.

If a LT GaN nucleation layer is used, one way of creating an uniform gable would be to grow for a much longer time at 1050°C before transitioning to the 950°C gable growth, imitating recipes used for planar films. However, the depth of the trench limits the growth time, and eliminating the gable altogether would not provide the dislocation turning over the post that makes the cantilever epitaxy method viable for achieving low-dislocation densities over large areas. Thus, it is necessary to figure out how to eliminate the steps, assuming that the potential exists to create some in each growth run. These experiments are conducted with the realization that it is not just the quality of the cantilevers as judged by the presence or lack of steps that matters, but also the way at which they coalesce.

Further growth on the wafer shown in Figure 24 reveals an additional interesting observation. Because the presence of $(11\bar{2}2)$ facets seems to be important to successful coalescence the growth conditions were modified to make sure that any additional growth emphasized their formation. To accomplish this, a subsequent growth was performed for 900 sec at 1030 °C. The growth was stopped at this point and the wafer examined by SEM in the same places as previous measurements. This showed small $(11\bar{2}2)$ facets as expected and something unexpected. The number of $(1\bar{1}01)$ steps was significantly reduced in areas of the highest density. The interesting part is that the growth conditions to produce $(11\bar{2}2)$ facets are also the growth conditions that seem to reduce the $(1\bar{1}01)$ steps; features that are known to be present when the undesirable surface discontinuities and dark-block defects occur at coalescence.

To test this even further and to hopefully coalesce the wafer with no dark-block defects and surface discontinuities, the wafer was put in the reactor for another growth at 1050 °C for 3600 sec. This growth did not coalesce the features but it did continue to reduce the number of $(1\bar{1}01)$ steps in each of the areas measured. Table 1 summarizes the reduction in steps for each area measured.

Table 1 shows a quantitative reduction in the number of $(1\bar{1}01)$ steps as growth proceeds in an effort to form $(11\bar{2}2)$ facets prior to coalescence.

AREA	Step density (number/cm^2)		
	First growth	Second growth	Third growth
	1080 °C (3600 sec)	1030 °C (900 sec)	1050 °C (3600 sec)
D2 (center)	3×10^4	4×10^4	3×10^3
D3 (R/2)	1×10^5	6×10^4	9×10^3
D4 (edge)	4×10^5	1×10^5	1×10^4

Because the features had still not coalesced the growth was continued for another 3600 sec at 1050 °C. At this point the wafer coalesced in some areas but not in others. After 5 growth runs the wafer was looking pretty ragged from particles generated by loading, unloading, and analysis. Based on other data from GNC0681A and the CV3000 series the coalescence will most likely have to be completed at a temperature higher than 1050 °C, but unfortunately this could not be completed on this wafer.

At this point further investigations will be needed to finalize the efforts described in this thesis and this will be discussed in the future direction section.

Chapter 5: Conclusions and Future Directions

5.1 Conclusions

GaN growth in general tends to be difficult to consistently reproduce. This holds true for all types of devices ranging from electronic to opto-electronic devices. Cantilever epitaxy is a good example of how the growth conditions for the nucleation layer and recovery portions of the film can vary dramatically with little change in the growth set points. These uncontrolled changes have a dramatic effect on the quality of a coalesced cantilever epitaxy film. Cantilever epitaxy is a good analogy for GaN growth in general. A lot of the irreproducibilities in device growth are most likely the result of changing reactor conditions at any stage in the process.

Cantilever epitaxy is sensitive to changes at all steps in the process. If the nucleation layer is not thick or dense enough the resultant gable will not be uniform. If the gable is not uniform, the quality of the overgrown cantilevers will be poor. If the quality of the overgrown cantilevers is poor then the coalescence is poor. In addition, just because the quality of the gable and overgrown cantilevers seems good, as in the experiments with an AlN buffer layer, the coalesced film can still be plagued with large non-radiative dark-block defects.

There are many factors that have to be right to produce viable cantilever epitaxy substrates. Some areas that have been identified are the need to have uniform gables for dislocation turning on top of the post, overgrown cantilevers without $(1\bar{1}01)$ steps, and coalescence with $(11\bar{2}2)$ facets. Although these three things seem necessary, the perfect

combination of growth steps has not yet been identified to reproduce the demonstrated successful substrates.

Silicon doping also seems to play a role in the quality of the coalesced substrate. There is no data in the literature to suggest that silicon significantly changes the growth kinetics, and studies to specifically test this have not been performed. There is some evidence that dopants in general, and silicon in particular affect the stress in the film during growth and this may be contributing to the coalescence problems. In addition, the ELO growths from which the kinetic data was derived are probably highly silicon doped. There is good evidence that the dielectric masks commonly used, incorporate at least as much silicon as intentional doping, on the order of 10^{18} cm^{-3}.

5.2 Future directions

5.2.1 Ga diffusion length

The topic of the Ga diffusion length on the surface of sapphire is an interesting fundamental topic that, if known, would lead to a better understanding of the GaN growth process. Just as ELO is a good technique to study the reaction rates of the different predominate faces in GaN growth, the cantilever epitaxy technique might be a good way to study the Ga diffusion length as it relates to various growth conditions such as temperature.

As was shown in section 4.1 the growth conditions have an effect on the quality of the nucleation layer that can be grown on top of the posts. If it is assumed that the probability for a Ga atom to land on a 1 μm wide posts does not change with temperature and if it is also assumed that once a Ga atom makes its way to the trench it cannot return

to the top of the post a hypothesis can be developed for why higher temperatures make nucleating a LT GaN buffer layer on top of the post more difficult. One hypothesis is that at higher temperatures the Ga diffusion length on the surface is longer, thereby causing more of the Ga atoms that initially land on the top of the post to migrate off the top surface of the post into the trench before they can attach to a surface step. This migration off of the post creates a less dense nucleation layer.

Designing a cantilever epitaxy mask with a range of post widths could test this hypothesis. Wafers with this pattern could then be tested under a variety of growth conditions to probe the affect on the Ga diffusion length. This experiment would be incredibly time consuming and detailed, but would potentially provide valuable insight into Ga diffusion mechanisms.

5.2.2 $(1\bar{1}01)$ *step formation, evolution, and concave corners*

The interesting thing about the $(1\bar{1}01)$ steps that are formed on the laterally overgrown cantilever is that the junction between the $(1\bar{1}01)$ face and the (0001) face is a concave corner. The equilibrium Wulff shape for any crystal consists only of convex corners. In order to see concave corners one has to intentionally force them into existence. The equilibrium Wulff shape for GaN is a pyramid with six $(1\bar{1}01)$ facets. Unpublished experiments conducted by Mike Coltrin and myself explore a variety of concave geometries using an ELO technique. These experiments show interesting and unexpected facet behavior for concave corners. The concave corner seen along the cantilevers is one that cannot be produced by changing the mask orientations in ELO. Etching a trench into already grown GaN, and then regrowing in the trench could potentially duplicate this face combination. A controlled experiment where the growth

from this concave corner could be carefully monitored might help explain why the $(1\bar{1}01)$ steps disappear under growth conditions that also produce $(11\bar{2}2)$ facets.

The study of inward growing features also extends to the trenches that are seen in partially coalesced GaN films without dark-block defects. The trenches seen in Figure 23 look strikingly similar to features seen in the ELO experiments that force growth from concave corners. Figure 25 shows a plan-view SEM of an ELO feature where growth proceeded both in an inward direction and outward direction from an opening in a Si_3N_4 mask. The solid black lines that form two hexagons indicate the original opening in the dielectric. The trench in the middle of the feature is formed when two $(11\bar{2}2)$ facets approach each other. Upon analysis of the CE data, data from the study of inward growing features and other standard ELO data has been reexamined and some unnoticed trends appear. Facets in these two cases have a hard time coalescing, just like the cantilevers that had large $(11\bar{2}2)$ facets. The lateral growth rate slows down as the facets approach each other. Other ELO data of lines with $(11\bar{2}2)$ facets show the same behavior. ELO features experience a growth enhancement at the beginning of growth due to an excess amount of available precursors. These excess precursors experience gas-phase transport to the growing feature because they cannot deposit on the dielectric mask. The apparent slowing of growth rates for facets was always attributed to a reduction of the enhancement effect as the mask was covered. Because there are no excess precursors in cantilever epitaxy this slowing of the lateral growth rate must be due to some other phenomena that has not yet been discovered. This problem will require a reinvestigation of the ELO data already on hand and potentially some new experiments. How this all relates to the cantilever epitaxy substrates is to be seen. An enhanced

understanding of the fundamentals behind what controls this behavior will help improve the final quality and reproducibility of the cantilever epitaxy films.

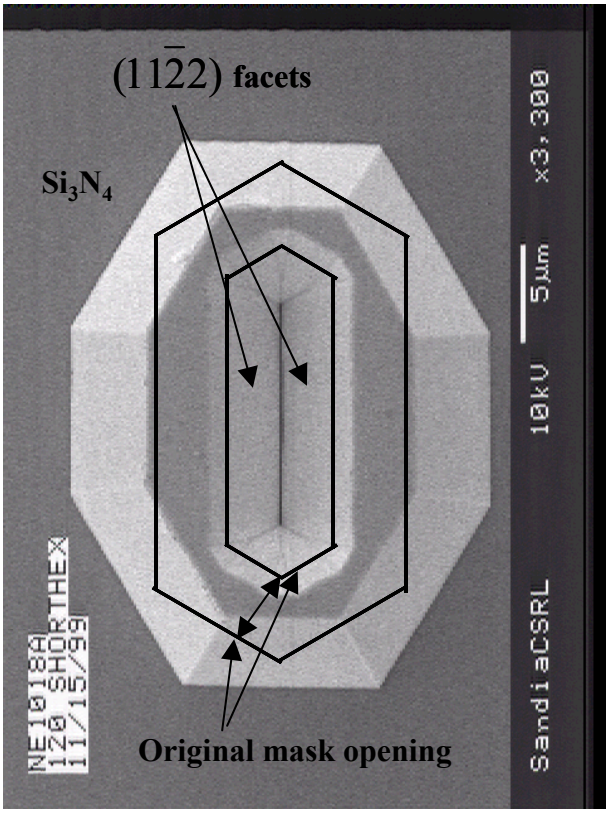

Figure 25. SEM of ELO feature where growth was forced to proceed from both concave and convex corners. The two facets coming together in the middle of the feature form a trench very similar to ones seen in partially coalesced CE films.

References

1. Nakamura, S. and G. Fasol, *The Blue Laser Diode*. 1997: Springer-Verlag Berlin Heidelberg. 343.

2. Koleske, D.D., et al., *In situ measurements of GaN nucleation layer decomposition.* Applied Physics Letters, 2003. **82**(8): p. 1170-1172.

3. Bhat, R., *Current Status of Selective Area Epitaxy by OMCVD.* Journal of Crystal Growth, 1992. **120**: p. 362-368.

4. Tanaka, T., et al., *Selective growth of gallium nitride layers with a rectangular cross-sectional shape and stimulated emission from the optical waveguides observed by photopumping.* Applied Physics Letters, 1996. **68**(7): p. 976.

5. Akasaka, T., et al., *GaN hexagonal microprisms with smooth vertical facets fabricated by selective metalorganic vapor phase epitaxy.* Applied Physics Letters, 1997. **71**(15): p. 2196.

6. Fini, P., et al., *High-Quality coalescence of laterally overgrown GaN stripes on GaN / sapphire seed layers.* Applied Physics Letters, 1999. **75**(12): p. 1706-1708.

7. Nakamura, S., et al., *InGaN/GaN/AlGaN-based laser diodes with modulation-doped strained-layer superlattices grown on an epitaxially laterally overgrown GaN substrate.* Applied Physics Letters, 1998. **72**: p. 211.

8. Linthicum, K., et al., *Pendeoepitaxy of gallium nitride thin films.* Applied Physics Letters, 1999. **75**(196): p. 196-198.

9. Ashby, C.I.H., et al., *Low-dislocation-density GaN from a single growth on a textured substrate.* Applied Physics Letters, 2000. **77**(20): p. 3233-3235.

10. Katona, T.M., et al., *Observation of crystallographic wing tilt in cantilever epitaxy of GaN on silicon carbide and silicon (111) substrates.* Applied Physics Letters, 2001. **79**(18): p. 2907-2909.

11. Strittmatter, A., et al., *Maskless epitaxial lateral overgrowth of GaN layers on structured Si (111) substrates.* Applied Physics Letters, 2001. **78**(6): p. 727-729.

12. Breiland, W.G. and K.P. Killeen, *A Virtual Interface Method for Extracting Growth Rates and High Temperature Optical Constants from Thin Semiconductor Films Using In Situ Normal Incidence Reflectance.* Journal of Applied Physics, 1995. **78**: p. 6726 - 6736.

13. Seager, C.H., et al., *Scanning cathodoluminescence as a probe of surface recombination in phosphors excited at low electron energies.* Journal of Applied Physics, 1997. **83**(2): p. 1153-1155.

14. Rosner, S.J., et al., *Correlation of cathodoluminescence inhomogeneity with microsturctural defects in epitaxial GaN grown by metalorganic chemical-vapor deposition.* Applied Physics Letters, 1997. **70**(4): p. 420-422.

15. Rosner, S.J., et al., *Cathodoluminescence mapping of epitaxial lateral overgrowth in gallium nitride.* Applied Physics Letters, 1999. **74**(14): p. 2035-2037.

16. Miyake, H., et al., *High Quality GaN Grown by Facet-Controlled ELO (FACELO) Technique.* Phys. Stat. Sol. (a), 2002. **194**(2): p. 545-549.

17. Sakai, A., et al., *Self-organized propagation of dislocations in GaN films during epitaxial lateral overgrowth.* Applied Physics Letters, 2000. **76**(4): p. 442-444.

18. Fini, P., et al., *Determination of tilt in the lateral epitaxial overgrowth of GaN using x-ray diffraction.* Journal of Crystal Growth, 1999. **209**(4): p. 581-590.

19. Katona, T.M., J.S. Speck, and S.P. DenBaars, *Control of crystallographic tilt in GaN grown on Si (111) by cantilever epitaxy.* Applied Physics Letters, 2002. **81**(19): p. 3558-3560.

Distribution:

10	MS 0601	C.C. Mitchell, 1126
1	MS 0601	A.A. Allerman, 1126
1	MS 0601	B.M. Biefeld, 1126
1	MS0601	K.H.A. Bogart, 1126
1	MS 0601	M.E. Coltrin, 1126
1	MS 0601	K.C. Cross, 1126
1	MS 0601	D.D. Koleske, 1126
1	MS 1056	D.F. Follstaedt, 1111
1	MS 1421	P.P. Provencio, 1122
1	MS 1415	N.A. Missert, 1112
1	MS 1415	G. Copeland, 1112
1	MS9018	Central Technical Files, 8945-1
2	MS0899	Technical Library, 9616